www.sciencemag.org/content/361/6399/285/suppl/DC1

Supplementary Materials for

Domain-focused CRISPR screen identifies HRI as a fetal hemoglobin regulator in human erythroid cells

Jeremy D. Grevet*, Xianjiang Lan*, Nicole Hamagami, Christopher R. Edwards, Laavanya Sankaranarayanan, Xinjun Ji, Saurabh K. Bhardwaj, Carolyne J. Face, David F. Posocco, Osheiza Abdulmalik, Cheryl A. Keller, Belinda Giardine, Simone Sidoli, Ben A. Garcia, Stella T. Chou, Stephen A. Liebhaber, Ross C. Hardison, Junwei Shi†, Gerd A. Blobel†

*These authors contributed equally to this work.
†Corresponding author. Email: jushi@upenn.edu (J.S.); blobel@email.chop.edu (G.A.B.)

Published 20 July 2018, *Science* **361**, 285 (2018)
DOI: 10.1126/science.aao0932

This PDF file includes:

Materials and Methods
Supplementary Text
Figs. S1 to S18
Tables S1 to S7
References

Other Supplementary Material for this manuscript includes the following:
(available at www.sciencemag.org/content/361/6399/285/suppl/DC1)

Data S1 to S5

Materials and Methods

Cell culture

HUDEP2 cells were cultured as described (*13*). Cells were maintained in StemSpan™ Serum Free Medium (SFEM, StemCell Technologies, Cat. #09650) supplemented with 50ng/ml human Stem Cell Factor (hSCF, Peprotech, Cat. #300-07), 10μM dexamethasone (Sigma, Cat. #D4902), 1μg/ml doxycycline (Sigma, Cat. #D9891), 3IU/ml erythropoietin (Amgen, Cat. #55513-144-10), 1% penicillin/streptomycin (ThermoFisher, Cat. #15140122). Cells were kept at a density of less than 1.0 million/ml. Differentiation was achieved by growing cells for 7 days (one medium change at day 3 or 4) in IMDM (Mediatech, Cat. #MT10016CV) supplemented with 50ng/ml hSCF, 3IU/ml erythropoietin, 2.5% fetal bovine serum, 250μg/ml holo-transferrin (Sigma, Cat. #T4132), 1% penicillin/streptomycin, 10ng/ml heparin (Sigma, H3149), 10μg/ml insulin (Sigma, Cat. #I9278), 1μg/ml doxycycline.

CD34+ cultures. Peripheral blood mononuclear cells (PBMCs) were obtained from the University of Pennsylvania Human Immunology Core. CD34+ cells were purified from using MACS MicroBead kit (Miltenyi, Cat #130-100-453) and cultured in three phases in IMDM supplemented with 3IU/ml erythropoietin, 2.5% human male AB serum (Sigma, Cat. #H4522), 10ng/ml heparin, 10μg/ml insulin. Phase-I medium was supplemented with 100ng/ml hSCF, 5ng/ml IL-3 (Peprotech, Cat. #200-03), 250μg/ml holo-transferrin. Phase-II medium was supplemented with 100ng/ml hSCF and 250μg/ml holo-transferrin. Phase-III medium was supplemented with 1.25mg/ml holo-transferrin. Cells were maintained in Phase-I from the day of collection until day 8. Cells were spin-infected (see virus preparation and infections below for full details) and transitioned to Phase-II media, and finally transitioned to Phase-III media on day 13 of culture. RNA samples for RT-qPCR were harvested on day 13 of culture for optimal RNA yield. Western Blot, HPLC, and HbF FACS samples were harvested on day 15 of culture.

Cell lines for sgRNA-scaffold optimization. A-375 cells were cultured in DMEM, HCT116 and A549 cells were cultured in DMEM/F-12, K562 cells were cultured in RPMI1640. All cell lines used in this study were mycoplasma free.

Plasmids

The Cas9 expression vector was constructed by inserting the 5′-3xFLAG-tagged human-codon optimized Cas9 cDNA from *Streptococcus pyogenes* (Addgene: #49535) into a lentiviral EFS-Cas9-P2A-Puro expression vector (made available at Addgene; #108100) using the In-Fusion cloning system (Clontech: #638909). All sgRNA encoding oligonucleotides were inserted into a lentiviral U6-sgRNA2.1-EFS-GFP expression vector (made available at Addgene: # 108098) using a BsmBI restriction site. Oligonucleotides corresponding to the shRNAs were annealed and cloned into the same vector as were sgRNAs with the sgRNA scaffold removed by a BsmBI-EcoRI double digestion resulting in LRG-U6-shRNA-EFS-GFP. See Table S4 for a list of shRNA sequences used for this study (sequences for shRNAs were obtained from the Broad Insitute Gene Perturbation Platform website https://portals.broadinstitute.org/gpp/public/).

Virus preparation and infections

Virus was produced in HEK293T cells grown in DMEM supplemented with 10% Fetal Bovine Serum, 2% penicillin/streptomycin, 1% L-glutamine, 100μM sodium pyruvate. HEK293Ts were plated in 10cm plates 18-24h prior to transfection such that cells were 90-100% confluent by the time of transfection. Expression vectors were mixed in a 4:3:2 ratio with packaging plasmids, PAX2, and VSVG envelope plasmid, respectively, in 500μl OPTI-MEM (ThermoFisher Scientific, Cat #31985070), and added to 500μl of 160μg/ml polyethylenimine (PEI, Polysciences Cat. #23966) in OPTI-MEM for precipitation. Plasmid precipitations were added to HEK293T cells and transfections were incubated at 37°C, 5% CO_2 for 6 hours, after which fresh media was placed on the cells. Viral supernatants were harvested 24 hours and 48 hours post-transfection and pooled.

One million HUDEP2 cells were infected with Cas9- or single sgRNA-containing virus by spin-infection with 1ml of viral supernatant supplemented with 8μg/ml polybrene and 10mM HEPES buffer. Spin-infections were carried out at 2,250 rpm for 1.5 hours at room temperature in 12-well plates. HUDEP2-Cas9 cells were selected starting 48-hours post-infection for 5 days in 1μg/ml puromycin. sgRNAs were transduced consistently above 90% GFP+ levels. See below for full details on transductions for the kinase domain sgRNA-library.

For infection of primary CD34+ derived erythroid cells with shRNA containing virus, viral particles required concentration due to lower infectivity of these cells. Viral supernatants were concentrated with LentiX-concentrator (Clontech, Cat. #631232) per manufacturer specifications. Viral pellets were resuspended in Phase-I media. Cells were spin-infected with concentrated virus from one 10cm plate (24-hour and 48-hour viral supernatants pooled) supplemented with 8μg/ml polybrene and 10mM HEPES per 1 million cells. Spin-infections were carried out at 2,250rpm for 1.5 hours at room temperature in 12-well plates, followed by incubation at 37°C, 5% CO_2 overnight. Cultures were then transitioned to Phase-II media.

TIDE analysis

CRISPR-Cas9 targeted regions were amplified by PCR from genomic DNA (gDNA) from HUDEP2 cells transduced with a sgRNA, as well as from an uninfected HUDEP2 control cell line. Primers were designed to flank targeted regions 250-300bp on either side. Amplifications were done with AccuPrime™ Pfx Supermix (ThermoFisher Scientific Cat. #12344040) per manufacturer specifications. Amplicons were purified with the QIAquick PCR purification kit (Qiagen, Cat. #28106), and Sanger sequenced at the Children's Hospital of Philadelphia sequencing core (NAPCore facility). Sequencing chromatograms were analyzed with the TIDE R-package (*22*). See Table S5 for a list of primers used for TIDE.

HbF flow cytometry and FACS

For HbF analysis cells were fixed in 0.05% glutaraldehyde for 10min, washed 3 times with PBS/0.1%BSA (Sigma, Cat. #A7906), and permeabilized with 0.1% Triton X-100 (Life Technologies Cat. #HFH10, prepared in PBS/0.1%BSA) for 5 minutes. Following one wash with PBS/0.1% BSA, cells were stained with HbF-APC conjugate antibody (Invitrogen, Cat. #MHFH05). For HUDEP2 samples, 2 to 5 million cells were incubated with 2μg HbF-APC antibody for 30 minutes in the dark at room temperature.

For primary CD34+ erythroid cells, 2 to 5 million cells were incubated with 0.4μg HbF-APC antibody for 10 minutes in the dark at room temperature. Cells were then washed twice with PBS/0.1%BSA. Flow cytometry was carried out on a BD FACSCanto™ and cell sorting on a BD FACSJazz™ at the Children's Hospital of Philadelphia flow cytometry core.

Kinase domain-focused CRISPR sgRNA library construction

A comprehensive human kinase gene list was taken from a previous study (*11*), and catalytic enzymatic domains retrieved from the NCBI database of conserved domain annotations. sgRNAs were designed against 496 kinase domains of 482 kinase genes, with 6 sgRNAs per domain. 26 sgRNAs targeting essential genes and 50 non-targeting sgRNAs were spiked-in as positive and negative controls, respectively. In total, the library contains 3052 sgRNAs. All the sgRNAs were designed using design principles previously reported and were filtered based on predicted off-target effects (*23*). sgRNAs were synthesized in a pooled format on an array platform (Twist Bioscience) and then PCR cloned into the LRG vector with sgRNA2.1 backbone (LRG 2.1 vector, see Supplementary Text for full description). To ensure proper representation of sgRNAs in the pooled lentiviral plasmids, the library was analyzed by deep-sequencing on a MiSeq instrument (Illumina), which confirmed that 100% of the designed sgRNAs were cloned in the LRG2.1 vector with over 95% of sgRNAs being within 5-fold of the mean read count.

CRISPR-Cas9 screen

The kinase domain-focused sgRNA library was packaged in lentivirus as indicated above. Viral titer was determined by serial dilution. HUDEP2-Cas9 cells were transduced with the kinase-domain library at a low multiplicity of infection (MOI 0.3-0.5) such that 30 to 50% of cells were GFP positive (MOI for these studies was of ~0.4, see Fig. S2E). 9 million cells were infected in total to yield 1000x coverage of the sgRNA library in the GFP+ population. GFP+ cells were sorted by FACS on day 2 post-infection.

GFP+ cells were then cultured in HUDEP2 media (as indicated above) for an additional 6 days (total 8 days post-infection). On day 8 post-infection, cells were transitioned to differentiation media (as indicated above), and differentiated for 7 days. On day 15 post-infection, cells were stained for HbF as indicated above, and sorted into HbF high and HbF low populations (see Fig. 1B) as previously described (*14*).

Genomic DNA (gDNA) was harvested from these samples by phenol/chloroform (Fisher Scientific Cat #BP1752I-100) extractions per standard methods. sgRNAs were amplified with Phusion Flash High Fidelity Master Mix Polymerase (ThermoFisher Scientific, Cat. #F-548L) per manufacturer specifications with the LRG F2/R2 primer pair (see Table S6). Reactions were done with 23 cycles of amplification with 100ng of gDNA, and 50 parallel reactions were performed to maintain sgRNA library representation. PCR reactions were then pooled for each sample and column purified with QIAGEN PCR purification kit. PCR products were subjected to Illumina MiSeq library construction and sequencing. First, PCR products were end repaired with T4 DNA polymerase (New England BioLabs, NEB), DNA polymerase I (NEB), and T4 polynucleotide kinase (NEB). Then, an A-overhang was added to the end-repaired amplicons using Klenow DNA Pol Exo- (NEB). The A-overhang DNA fragment was ligated with diversity-increased barcoded Illumina adaptors followed by seven pre-capture PCR cycles with primer pair

PE-5/PE-7 (see Table S6). Samples were then purified with the QIAquick PCR purification kit. sgRNA library concentrations were quantified on a 2100 Bioanalyzer (Agilent). The barcoded libraries were pooled at an equal molar ratio and subjected to massively parallel sequencing through a MiSeq instrument (Illumina) using 75-bp paired-end sequencing (MiSeq Reagent Kit v3; Illumina MS-102-3001).

The sequencing data were de-barcoded and trimmed to contain only the sgRNA sequence, and subsequently mapped to the reference sgRNA library without allowing any mismatches. The read counts were calculated for each individual sgRNA and normalized to total read counts. Normalized read counts of sgRNAs in HbF high and HbF low populations were $\log_2$ transformed in R, and graphical representation was done using the R-package ggplot2. To exclude false positives due to off-target effects or inconsistencies in sample preparation, we only focused on kinases for which multiple sgRNAs were enriched.

Western Blot

Western blotting was performed using standard procedures. Primary antibodies: HRI (1:1000, Biosource, Cat. #MBS2526743), eIF2α-Phospho (1:1000, anti-EIF2S1-phospho-S51, Abcam, Cat. #ab32157), total-eIF2α (1:1000, Cell Signaling, Cat. #9722), BCL11A (1:1000, Abcam, Cat. #19489), LRF (1:1000, eBioscience Cat. #), GATA1 (1:1000, Santa Cruz, Cat. #sc-265), γ-globin (1:1000, Santa Cruz, Cat. #sc-21756), B-actin (1:1000, Santa-Cruz, Cat. #sc-47778). Secondary antibodies: anti-rabbit (1:10,000, GE Healthcare, Cat. #NA934V); anti-mouse (1:10,000, GE Healthcare, Cat. #NA931V).

RT-qPCR

RNA samples were harvested in TRIzol™ (ThermoFisher Scientific, Cat #15596018), and purified with the RNeasy Mini kit which included an on-column DNAse treatment to remove genomic DNA (Qiagen, Cat. #74106). cDNAs were prepared by reverse-transcription using iScript Supermix (Bio-Rad, Cat. #1708841). qPCR reactions were prepared with Power SYBR Green (ThermoFisher Scientific) and run on a ViiA7 Real Time qPCR machine (ThermoFisher Scientific). Quantification was performed with the ΔΔCT method. Data were normalized to LRF as it was unperturbed across conditions and we found it to be more stable during erythroid maturation than housekeeping genes such as B-actin, but results were robust to normalization against such other transcripts as well. Primers used for RT-qPCR are listed in Table S7.

RNA-seq

Total RNA was harvested in TRIzol™, and purified with the RNeasy Mini kit including a DNase treatment step to remove genomic DNA. Sequencing libraries were then constructed from 100 ng of purified total RNA using the ScriptSeq Complete Kit (Illumina cat# BHMR1224) according to manufacturer's specifications. In brief, the RNA was subjected to rRNA depletion using the Ribo-Zero removal reagents and fragmented. First strand cDNA was synthesized using a 5' tagged random hexamer, and reversely transcribed, followed by annealing of a 5' tagged, 3'-end blocked terminal-tagged oligo for second strand synthesis. The Di-tagged cDNA fragments were purified, barcoded, and PCR-amplified for 15 cycles.

The size and quality of each library were then evaluated by Bioanalyzer 2100 (Agilent Techniologies, Santa Clara, CA), and quantified using qPCR. Libraries were sequenced in paired-end mode on a NextSeq 500 instrument to generate 2 x 76 bp reads using Illumina-supplied kits. The sequence reads were processed using the ENCODE3 long RNA-seq pipeline (https://www.encodeproject.org/pipelines/ENCPL002LPE/). In brief, reads were mapped to the human genome (hg19 assembly) using STAR, followed by RSEM for gene quantifications. Read counts were further analyzed with the R-package DESeq2.

Proteomics analysis via nLC-MS/MS

Cells were lysed in 100µl of cold lysis buffer (6M urea/2M thiourea, 50 mM ammonium bicarbonate, pH 8.0). Dithiothreitol (DTT) was added to a final concentration of 5 mM for 1 hour at room temperature and alkylated with 20 mM iodoacetamide in the dark for 30 minutes at room temperature. Samples were diluted 5x to reduce urea concentration. Proteins were then digested with trypsin (Promega) at an enzyme-to-substrate ratio of approximately 1:50 overnight at room temperature. Digestion was interrupted by adding 1% trifluoroacetic acid. Samples were desalted using Sep-Pak tC18 Plus Light Cartridge (Waters). The peptide samples were subsequently lyophilized.

Dried samples were resuspended in buffer A (0.1% formic acid) and loaded onto an Easy-nLC system (Thermo Fisher Scientific, San Jose, CA, USA), coupled online with a Q-Exactive mass spectrometer (Thermo Scientific). Peptides were loaded into a picofrit 18 cm long fused silica capillary column (75 µm inner diameter) packed in-house with reversed-phase Repro-Sil Pur C18-AQ 3 µm resin. A gradient of 105 minutes was set for peptide elution from 2-28% buffer B (100% ACN/0.1% formic acid), followed by a gradient from 28-80% buffer B in 5 min and an isocratic 80% B for 10 min. The flow rate was 300 nl/min. The MS method was set up in a data-dependent acquisition (DDA) mode. The full MS scan was performed at 70,000 resolution (FWHM at 200 *m/z*) in the *m/z* range 360-1200 and an AGC target of 10e6. Tandem MS (MS/MS) was performed at a resolution of 17,500 with an HCD collision energy set to 24, an AGC target of 2x10e4, a maximum injection time to 100 msec, a loop count of 10, an intensity threshold for signal selection at 10e4, including charge states 2-4, and a dynamic exclusion set to 60 sec.

MS raw files were analyzed by MaxQuant software (*24*) version 1.5.5.1. MS/MS spectra were searched by the Andromeda search engine against the Human UniProt FASTA database (version November 2015). All parameters for the search were kept as default. Intensity-based absolute quantification (iBAQ) was enabled for label-free quantification. Match between runs was enabled and set to 1 min window.

For data analysis, iBAQ values were $\log_2$ transformed and normalized by subtracting to each value the average value of the respective sample. Statistics was performed by using a two-tailed homoscedastic t-test.

Hemoglobin HPLC

Cell were lysed in MilliQ H_2O. Hemolysates were cleared by centrifugation and analyzed for identity and levels of hemoglobin variants (HbF and HbA) by cation-exchange high-performance liquid chromatography (HPLC). We utilized a Hitachi D-7000 Series (Hitachi Instruments, Inc., San Jose, CA), and a weak cation-exchange column (Poly CAT A: 35 mm x 4.6 mm, Poly LC, Inc., Columbia, MD). Hemoglobin isotype peaks were eluted with a linear gradient of phase B from 0% to 80% at A_{410nm} (Mobile Phase A: 20

mM Bis-Tris, 2 mM KCN, pH 6.95; Phase B:20 mM Bis-Tris, 2 mM KCN, 0.2 M sodium chloride, pH 6.55). Cleared lysates from normal human cord blood samples (high HbF content), as well as a commercial standard containing approximately equal amounts of HbF, A, S and C (Helena Laboratories, Beaumont, TX), were utilized as reference isotypes.

Sickling assay

Cells were resuspended in 100μL HEMOX buffer supplemented with glucose (10 mM) and BSA (0.2 %) in a 96-well plate. Suspensions were subsequently incubated under Nitrogen gas at 37°C for 1 hour. 200μL of 2% glutaraldehyde solution was then added to the samples without exposure to air for immediate fixation. Fixed cell suspensions were spread onto glass microslides (Fiber Optic Center) and subjected to microscopic morphological analysis of bright field images (at 40x magnification) of single layer cells on an Olympus BX40 microscope fitted with an Infinity Lite B camera (Olympus), and the coupled Image Capture software. Images were randomized and blinded. The percentage of sickled cells for each condition was obtained by manually counting the number of sickled cells.

Wright-Giemsa stains

Cells were spun onto glass slides with a Cytospin4 (ThermoFisher Scientific, Cat#A78300003) at 1,000rpm for 3 min. Slides were allowed to dry for 5 minutes before staining with May Grünwald (Sigma Aldrich, MG1L-1L) for 2 minutes followed by 1:20 diluted Giemsa stain (Sigma Aldrich, GS-500 500ML) for 10 minutes. The stained slides were rinsed in water and allowed to dry for 10 minutes before a coverslip was sealed on the preparation with Cytoseal 60 (Thermo Scientific Cat #8310-4). The images were captured at 10X resolution on Olympus BX60 microscope using Infinity software (Lumenera corporation).

Polysome profiling

Cells were arrested in Phase II media with 100ug/ml cycloheximide (Sigma CC4859) for 15 minutes at 37C. Cells were then washed twice in ice cold 1x PBS with 100ug/ml cycloheximide, and resuspended in 500ul lysis buffer (10mM Tris-HCl (pH 7.4), 5mM MgCl2, 100mM KCl, 1% Triton X-100, 2mM DTT, 500U/mL RnasinPlus (Promega N2615), protease inhibitor cocktail (Sigma 11873580001)). Lysates were then dounced with a 26G needle 5 times, and cellular debris were cleared by centrifugation at 13,000rpm for 10 minutes. 10% of cleared lysates were set aside for input mRNA quantitation, and samples were snap-frozen in liquid nitrogen.

Cleared polysomal lysates were loaded on sucrose gradients and spun at 40,000rpm for 2 hours at 4C (Beckman SW41 rotor). Sixteen fractions of equal volume (~700ul) were collected and gradient profiles were measured by ultraviolet absorbance at 254nm with a UA-5 detector (ISCO). Fractions were incubated with 1% SDS and proteinase K for 30 minutes at 37C, and stored at -80C until further analysis.

RNA was purified from fractions by phenol-chloroform extraction. ERCC spike-in RNA was added to each fraction (1ul of 1:10 dilution of spike-in control per fraction, ERCC-spike in (ThermoFisher, 4456740)). 400ul of phenol (Phenol/Water 3.75:1 Invitrogen Cat. # 15594-047) was added to each fraction. Samples were vortexed for 30 seconds. 350ul of chloroform (ThermoFisher, Cat. #BP1145-1) was added, and samples

were vortexed again for 30 seconds. Samples were spun down at 10,000rpm for 10 minutes, and aqueous layers were transferred to fresh tubes. One additional round of phenol-chloroform extractions were performed. Aqueous phases were split into two tubes with 350ul of sample each. 1.5ul of glycogen carrier, 30ul of 3M sodium acetate pH 5.5 (ThermoFisher, Cat. #AM9740) and 800ul of ice cold 100% ethanol were added to each final aqueous phases, and place at -80C overnight. RNA was precipitate by spinning samples at 13,000rpm for 30 minutes at 4C. Pellets were washed with 1mL of 75% ethanol, and RNA was resuspended in nuclease-free water. cDNAs were prepared using iScript Supermix (Bio-Rad, Cat. #1708841). qPCR reactions were prepared with Power SYBR Green (ThermoFisher Scientific) and run on a ViiA7 Real Time qPCR machine (ThermoFisher Scientific).

BCL11A cDNA rescue experiments

The BCL11A cDNA was a gift from Jian Xu (UT Southwestern) and subcloned into a lentiviral LRG-EFS-BCL11A-IRES-mCherry vector by In-Fusion cloning. Virus was prepared and transduced in respective cell lines as indicated above. To control for expression levels, the low 50% mCherry+ cells were sorted on a BD FACSJazz™ at the Children's Hospital of Philadelphia flow cytometry core. Cells were differentiated and analyzed as indicated above.

Mouse fetal liver cultures

E14.5 mouse fetal livers were obtained from CD1 pregnant females (Charles River strain code 022, req #V00018219:1, IACUC protocol #660). The EasySep™ Mouse Hematopoietic Progenitor Cell Enrichment Kit (Stem Cell Technologies cat. #19756) was used for hematopoietic progenitor isolation. Cells were transduced with shRNAs per spinfection protocol detailed above. Transduced cells were cultured for 48h in StemPro34 with supplement (Thermo Fisher cat #10639011), 1% L-glutamine, 1% P/S, 0.5U/ml erythropoietin, 1μM dexamethasone. Cells were harvested for RT-qPCR and Western Blot as indicated above.

Pomalidomide combination experiments

HUDEP2 cells were incubated with 10μM pomalidomide (Sigma, Cat. # P0018) for 2 days. Cells were then transitioned to differentiation media as indicated above for 7 days. During the course of differentiation cells were maintained in 10μM pomalidomide. Media was changed 3 to 4 days within the differentiation phase with fresh drug supplemented. HbF FACS and RT-qPCR were performed as indicated above.

Supplementary Text

<u>sgRNA scaffold optimization</u>

Prior to carrying out this screen we attempted to maximize editing efficiency by modifying the *Streptococcus Pyogenes* sgRNA scaffold. This sequence adopts a well-defined secondary structure, with a repeat-antirepeat duplex linked to a tetraloop and 3 stem loops, all of which facilitate binding to Cas9 and stabilize the sgRNA (Fig. S1A,B) (*25*). Previous work showed that an A-U flip in the repeat-anti-repeat duplex removes a putative premature Pol-III stop codon, and that extending the tetraloop significantly

improved sgRNA stability and Cas9 activity (*26*). By examining the Cas9 crystal structure, we noticed that stem loop 2 forms few contacts with Cas9 residues, similar to the tetraloop (*25*). Mutations in stem loop 2 are also well tolerated and allow for efficient Cas9 activity (*25*). We thus reasoned that extending stem loop 2 could further improve sgRNA stability similar to what had been done for the tetraloop, as this could further increase the double-stranded portion of the scaffold (Fig. S1B). We compared different lengths of such extensions (sgRNA 2.0 – sgRNA2.3).

To do so, we performed negative selection assays using the bicistronic sgRNA/GFP expression vector detailed above (LRG, Addgene: #65656). Cell lines were transduced with sgRNAs targeting essential genes such that selection against the sgRNAs would directly reflect editing efficiency for the different sgRNA scaffold designs. Negative selection was estimated by taking the proportion of GFP+ cells remaining over time (flow cytometry analysis was performed on 96-well plates of cells using a Guava Easycyte HT instrument (Millipore), gating was performed on live cells (using forward and side scatter), before measuring of GFP+ cells) (Fig. S1C,D). We found that an extended hairpin structure in both tetraloop and stem loop regions of the sgRNA backbone (termed sgRNA2.1) significantly improved the magnitude of negative selection in various human cell lines induced by sgRNAs targeting DNA replication proteins RPA3 and PCNA (Fig. S1C,D).

We then tested the modified scaffold design in HUDEP2 cells, a human erythroid cell line with low HbF background levels (See Materials and Methods for full details) (*17*) which we used to perform the kinase domain screen (Fig. S2A). Control sgRNAs targeting the known HbF regulators BCL11A and the chromatin remodeler CHD4 (*27*), were introduced via lentivirus into engineered HUDEP2 derivatives stably expressing Cas9 (HUDEP2-Cas9, see Materials and Methods for full details). Indel distributions were assessed by TIDE (see Materials and Methods for full details) (*22*). In the context of the sgRNA 2.1 template we achieved up to 98% editing efficiency as early as 4 days post-infection (Fig. S2B) with most sequence perturbations being deletions of less than 10 base pairs (Fig. S2C). As expected, targeting BCL11A increased the number of HbF positive cells (*14*). Based on these results, we used the sgRNA 2.1 design for all subsequent CRISPR-based experiments.

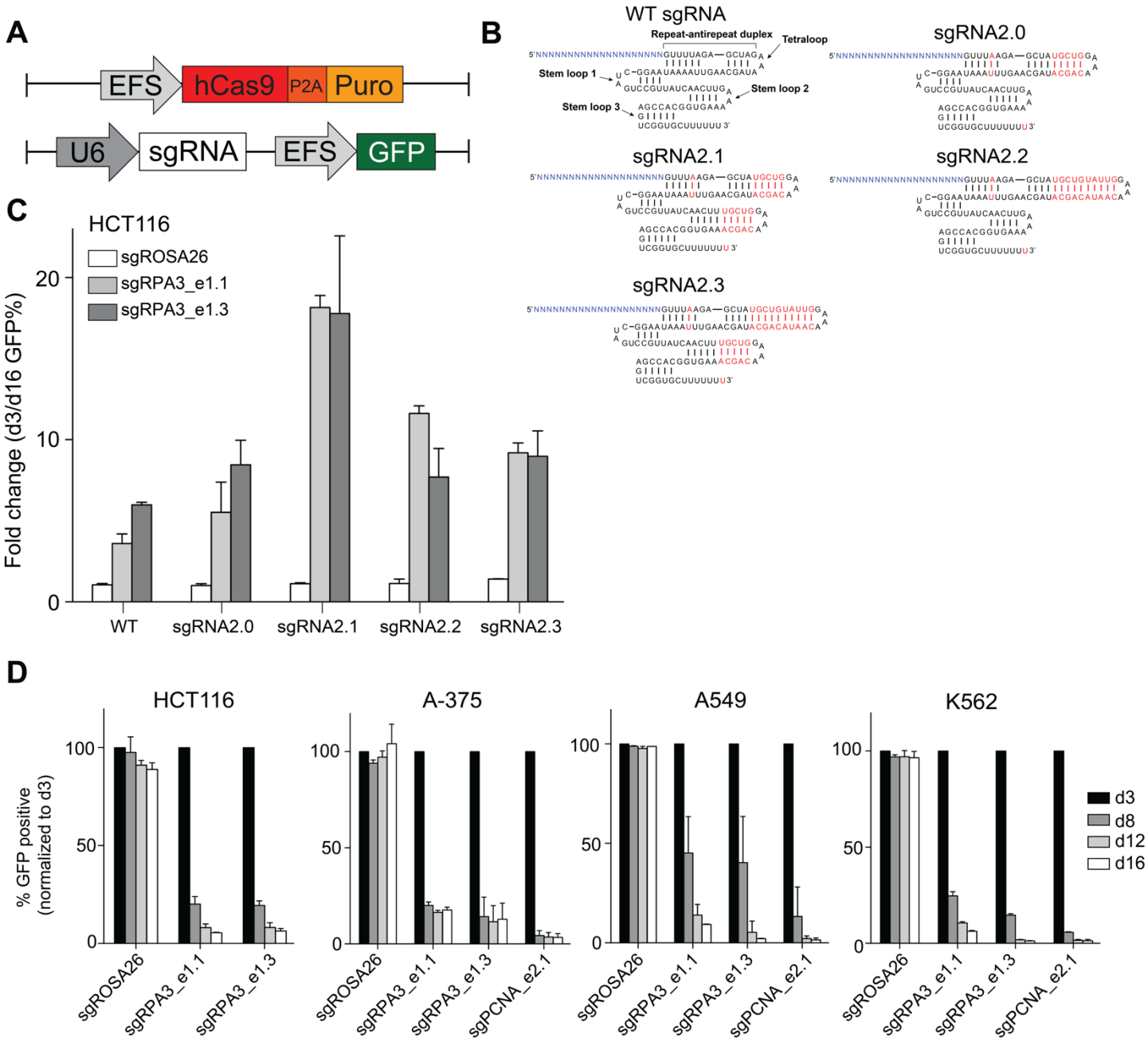

Fig. S1. sgRNA scaffold optimization. (See Supplementary Text for full description). (**A**) Cas9 and sgRNA plasmid designs. (**B**) sgRNA scaffolds tested, modifications to WT sgRNA-scaffold are highlighted in red. sgRNA 2.0 was previously described (*26*). (**C**) sgRNA editing efficiency assessed in HCT116 cells. GFP+ populations were measured at day 3 and day 16 post-sgRNA infection with sgRNAs targeting the essential DNA replication gene RPA3, and the ROSA26 locus as a negative control. Fold depletion was used to quantify editing efficiency for each of the sgRNA-scaffold designs. (**D**) sgRNA editing efficiency was similarly assessed with sgRNA-scaffold design 2.1 in HCT116, A-375, A549 and K562 cells lines. sgRNAs against the essential DNA replication genes RPA3 and PCNA were used, as well as an sgRNA targeting the ROSA26 locus as a negative control.

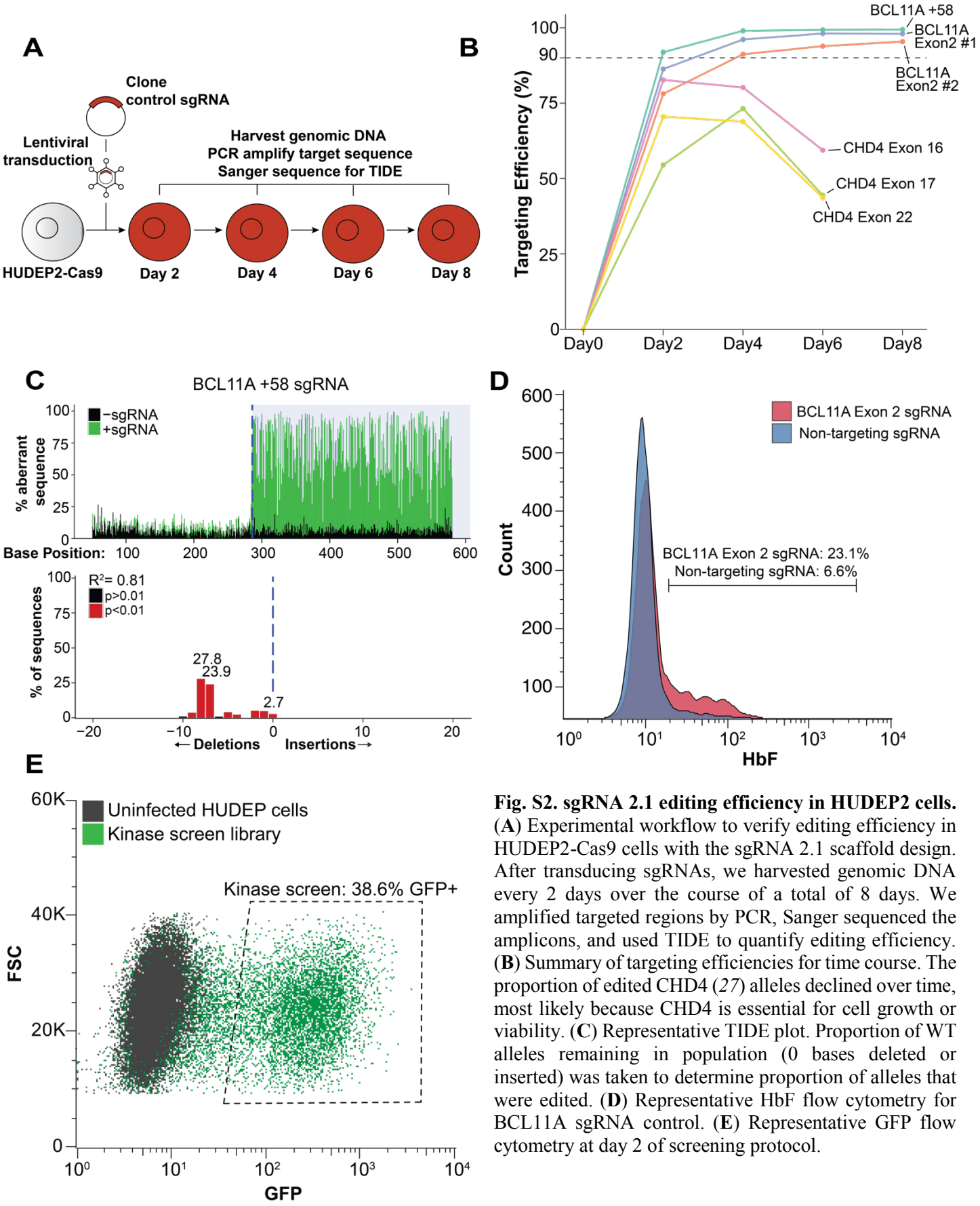

Fig. S2. sgRNA 2.1 editing efficiency in HUDEP2 cells. (**A**) Experimental workflow to verify editing efficiency in HUDEP2-Cas9 cells with the sgRNA 2.1 scaffold design. After transducing sgRNAs, we harvested genomic DNA every 2 days over the course of a total of 8 days. We amplified targeted regions by PCR, Sanger sequenced the amplicons, and used TIDE to quantify editing efficiency. (**B**) Summary of targeting efficiencies for time course. The proportion of edited CHD4 (*27*) alleles declined over time, most likely because CHD4 is essential for cell growth or viability. (**C**) Representative TIDE plot. Proportion of WT alleles remaining in population (0 bases deleted or inserted) was taken to determine proportion of alleles that were edited. (**D**) Representative HbF flow cytometry for BCL11A sgRNA control. (**E**) Representative GFP flow cytometry at day 2 of screening protocol.

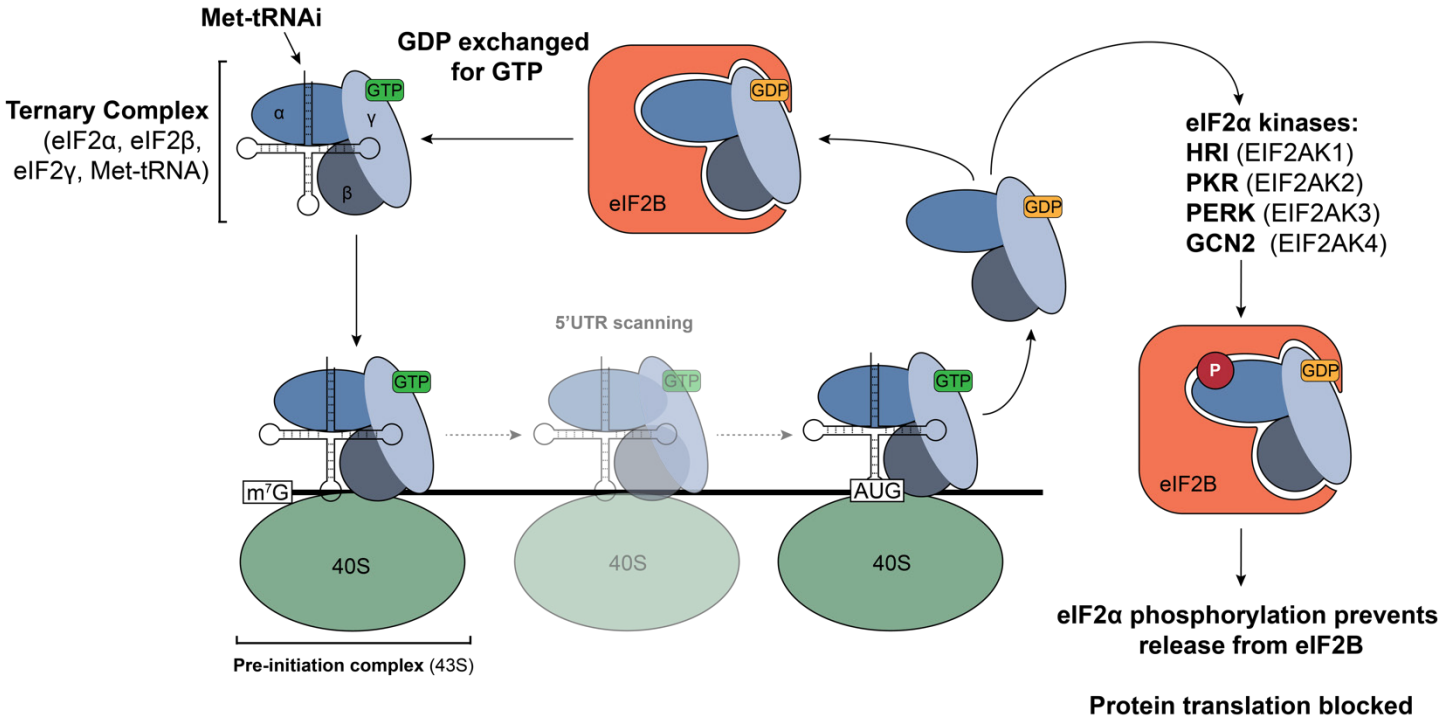

Fig. S3. HRI's role in regulating protein translation initiation. HRI is one of four kinases known to phosphorylate the protein translation initiation factor eIF2α (*15*). In its unphosphorylated form, eIF2α bound to GTP as part of a ternary complex with eIF2β and eIF2γ recruits the first methionine tRNA to the 40S ribosomal subunit to form a pre-initiation complex (PIC). The PIC then scans along the 5'UTR until it recognizes a start codon, at which point the GTP bound to eIF2α is hydrolyzed to GDP and the eIF2 factors are released from the PIC, allowing for formation of the 80S ribosomal unit. GDP is released from the eIF2 complex by the guanine exchange factor eIF2B, which allows for these factors to participate in further rounds of translational initiation. The phosphorylation of eIF2α prevents its release from eIF2B, thus blocking the recycling of this factor and further rounds of translation initiation. As such, the family of eIF2α kinases function as general repressors of protein translation.

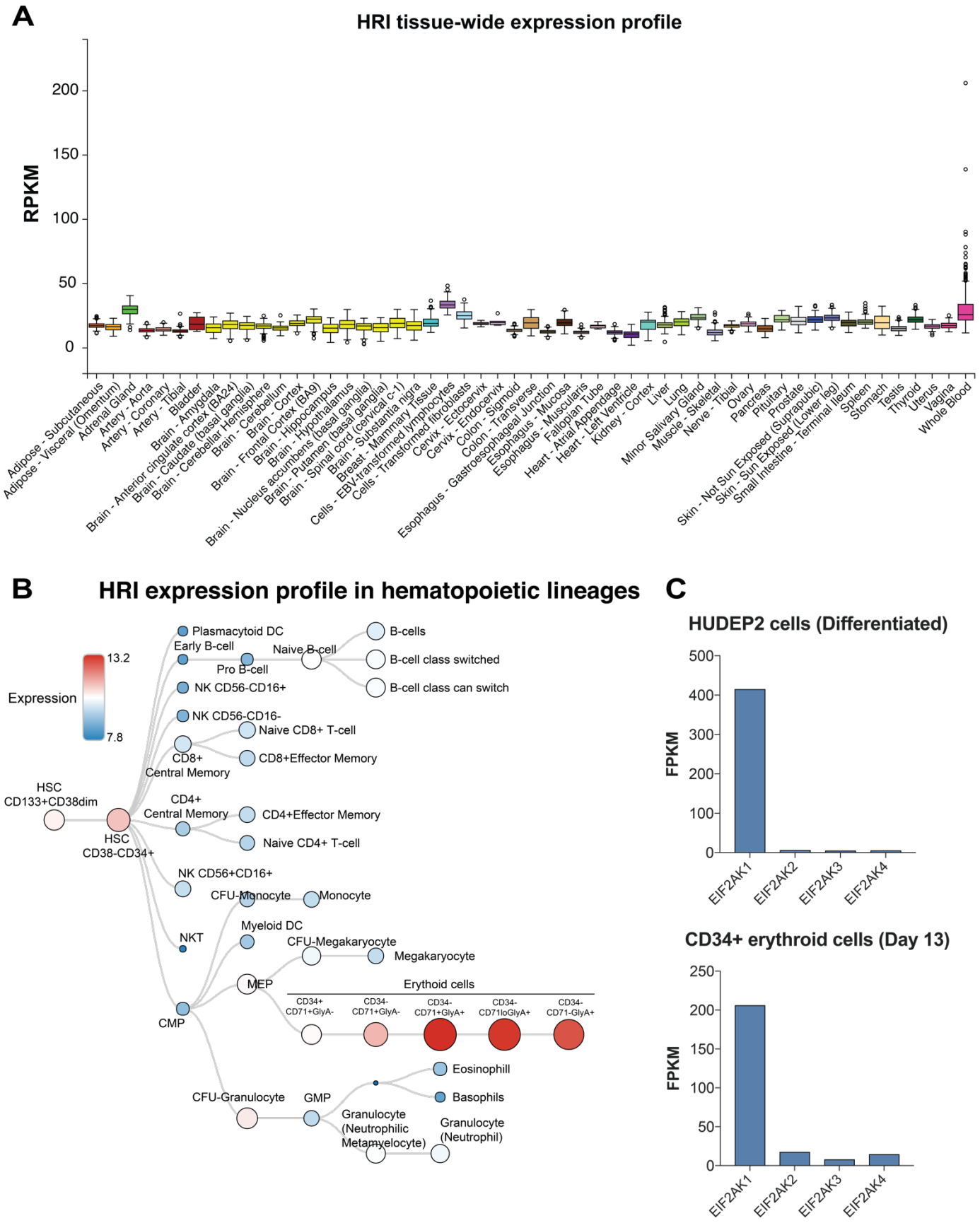

Fig. S4. Tissue expression for HRI. (**A**) Tissue-wide expression profile for HRI from GTEx. Expression levels for HRI are highest in whole blood. (**B**) Hematopoietic expression profile for HRI from BloodSpot (http://servers.binf.ku.dk/bloodspot/) (*28*). Expression levels for HRI are highest in the erythroid lineage. (**C**) Expression levels of eIF2α kinases in HUDEP2 cells and CD34+ erythroid cells. HRI is the highest expressed eIF2α kinase in these systems. It is worth noting that while the other eIF2α kinases were included in the CRISPR-screen shown in Fig. 1, they were not enriched in the HbF population, suggesting they are not expressed at high enough levels to impact on HbF induction.

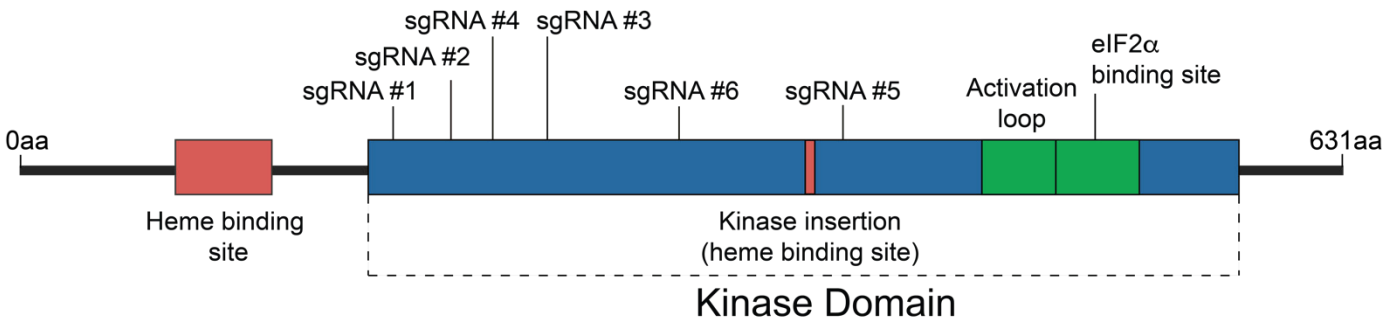

Fig. S5. HRI domain architecture. Position of the six "hit" HRI sgRNAs within the kinase domain.

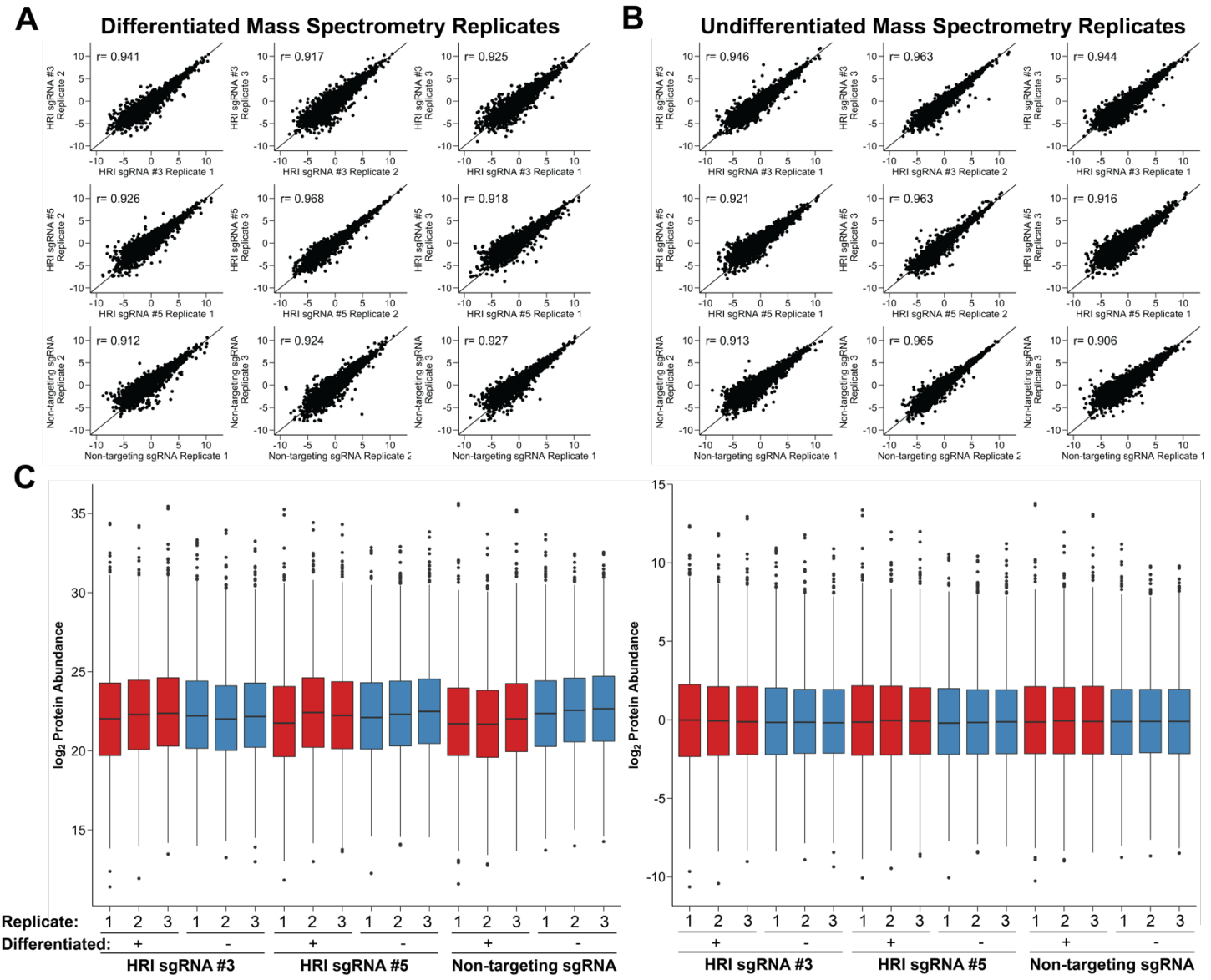

Fig. S6. Replicate concordance for mass spectrometry samples and normalization. (**A**) Replicate experiments in differentiated HUDEP2 cells. (n=3) biological replicates were generated each for HRI sgRNA #3, HRI sgRNA #5, and non-targeting sgRNA HUDEP2-Cas9 cell pools. All 3 pairwise replicate comparisons are shown for each condition. R-values denote Pearson correlation coefficients. Plots show $\log_2$ protein abundance for each replicate displayed. (**B**) Replicate experiments in undifferentiated HUDEP2 cells. (n=3) biological replicates were generated each for HRI sgRNA #3, HRI sgRNA #5, and non-targeting sgRNA HUDEP2-Cas9 pools. All 3 pairwise replicate comparisons are shown for each sample. R-values denote Pearson correlation coefficients. Plots show $\log_2$ protein abundance for each replicate displayed. (**C**) Normalization for mass spectrometry data. Protein abundances were $\log_2$ transformed (left panel), and normalized to their mean (right panel).

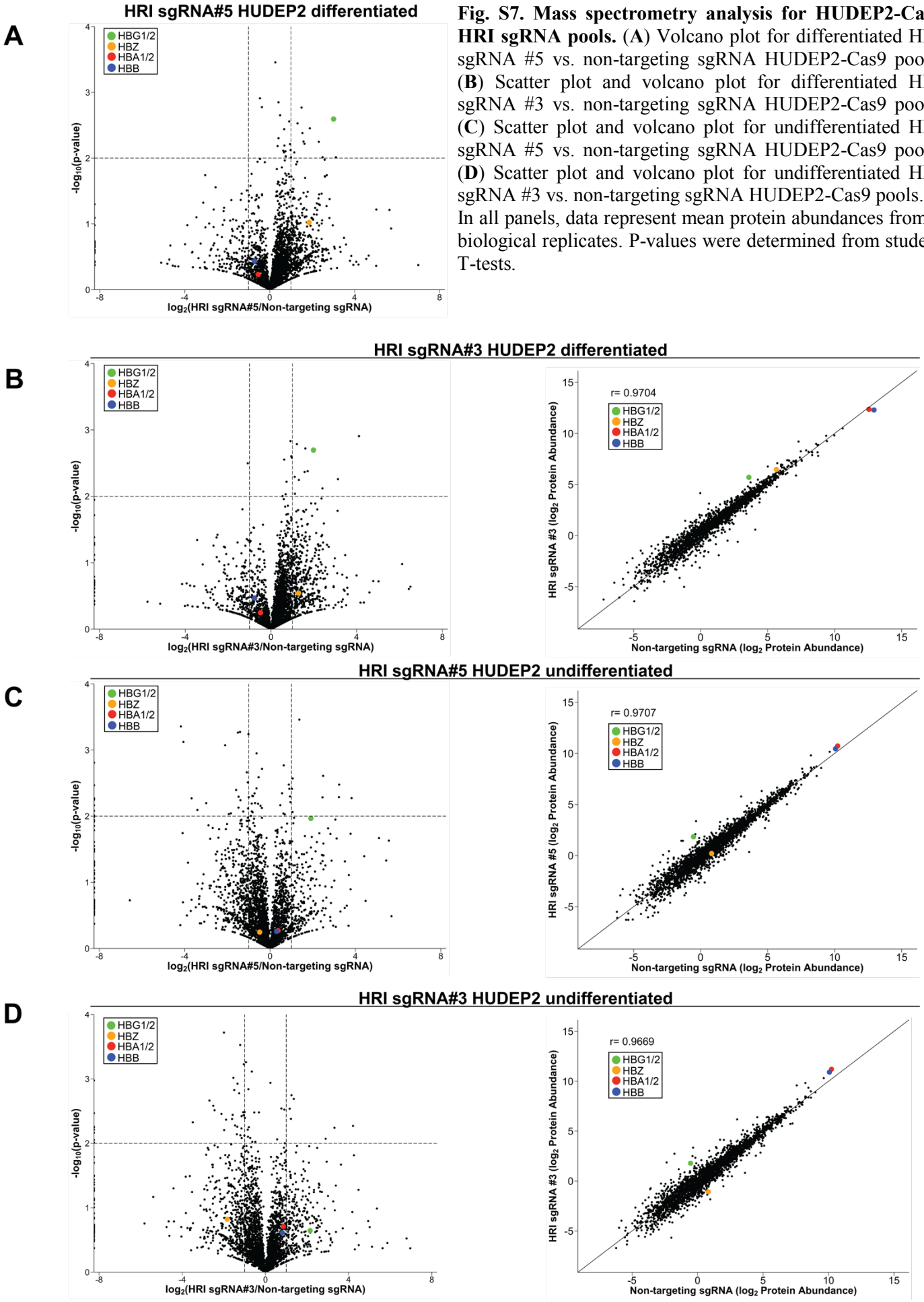

Fig. S7. Mass spectrometry analysis for HUDEP2-Cas9 HRI sgRNA pools. (**A**) Volcano plot for differentiated HRI sgRNA #5 vs. non-targeting sgRNA HUDEP2-Cas9 pools. (**B**) Scatter plot and volcano plot for differentiated HRI sgRNA #3 vs. non-targeting sgRNA HUDEP2-Cas9 pools. (**C**) Scatter plot and volcano plot for undifferentiated HRI sgRNA #5 vs. non-targeting sgRNA HUDEP2-Cas9 pools. (**D**) Scatter plot and volcano plot for undifferentiated HRI sgRNA #3 vs. non-targeting sgRNA HUDEP2-Cas9 pools. In all panels, data represent mean protein abundances from 3 biological replicates. P-values were determined from student T-tests.

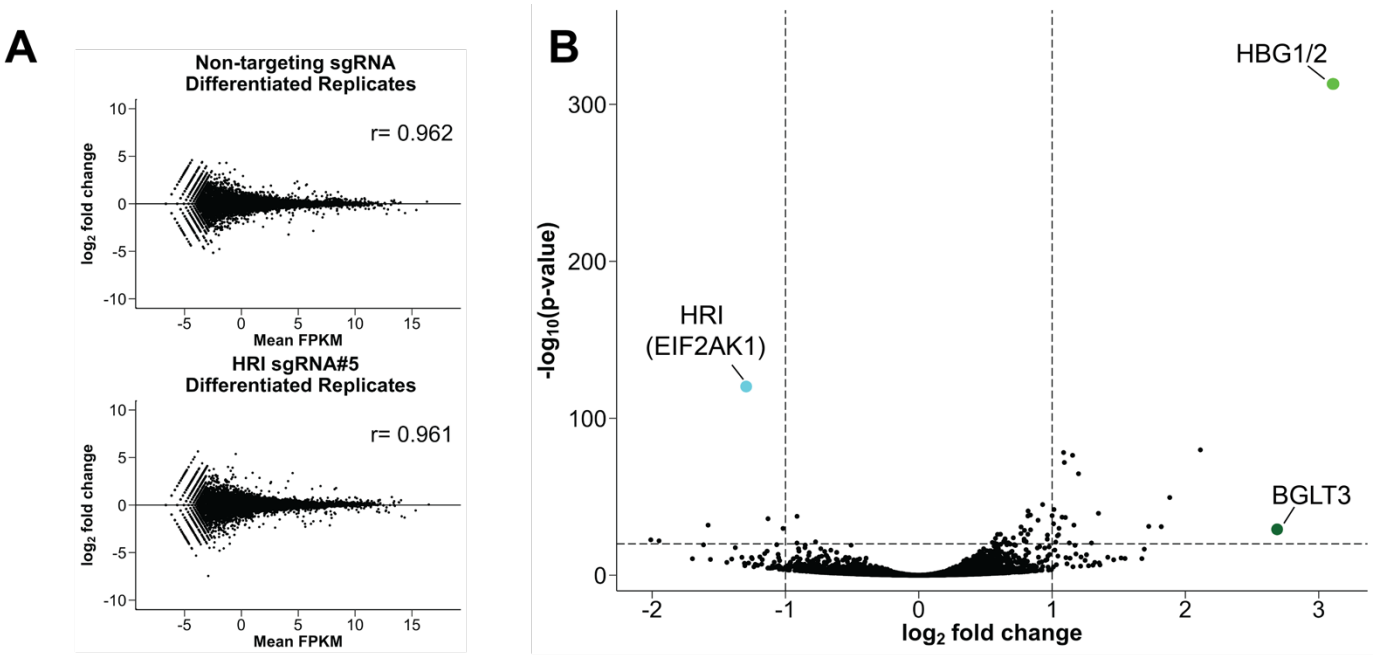

Fig. S8. RNA-seq for HUDEP2 cells. (**A**) MA plots for HRI sgRNA #5 and non-targeting sgRNA HUDEP2-Cas9 pools. 2 RNA seq biological replicates were generated each for differentiated cells. R-values denote Pearson correlation coefficients across the two indicated replicates. (**B**) Volcano plot for differentiated HRI sgRNA #5 and non-targeting sgRNA pools. Statistical significance was determined using the R-package DESeq2, with a negative binomial as a null distribution to determine statistical significance. P-values were FDR corrected for multiple hypothesis testing. Vertical lines denote 2 fold changes, and the horizontal line denotes a significance level of 10^{-20}.

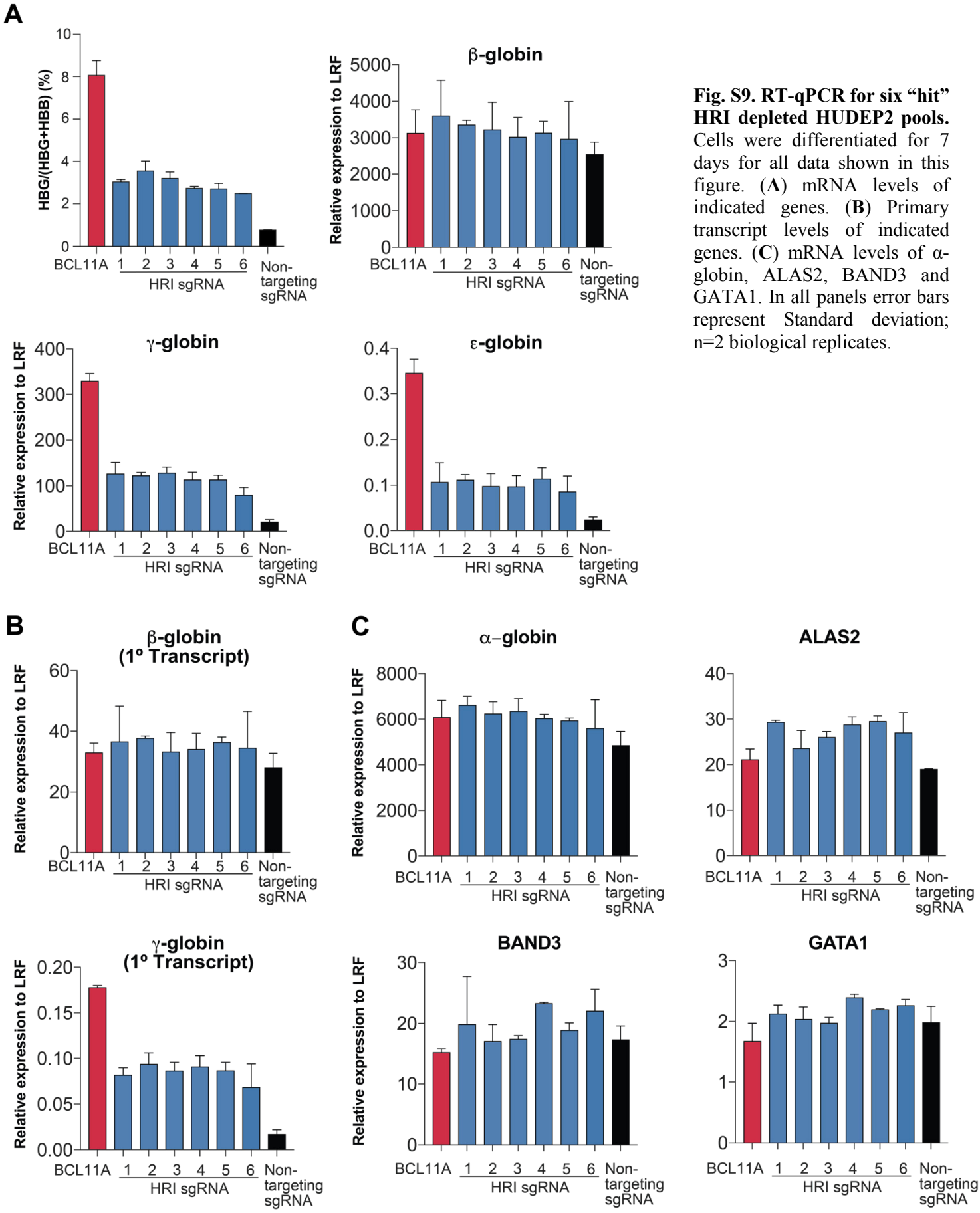

Fig. S9. RT-qPCR for six "hit" HRI depleted HUDEP2 pools. Cells were differentiated for 7 days for all data shown in this figure. (**A**) mRNA levels of indicated genes. (**B**) Primary transcript levels of indicated genes. (**C**) mRNA levels of α-globin, ALAS2, BAND3 and GATA1. In all panels error bars represent Standard deviation; n=2 biological replicates.

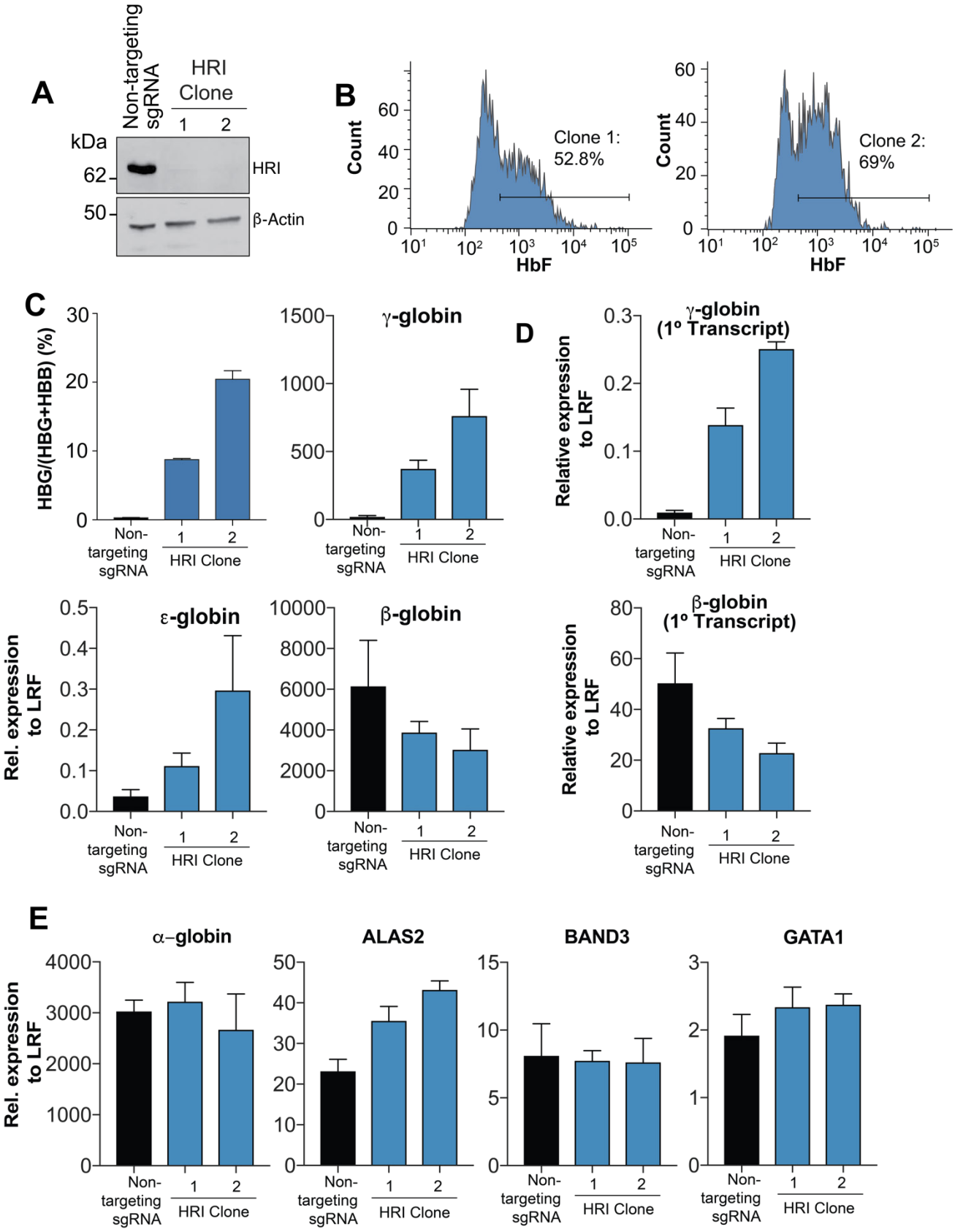

Fig. S10. HRI depleted HUDEP2 clones. Given the heterogeneity of mutations induced by sgRNAs in pools (see Fig. S2), we generated clonal HUDEP2 HRI depleted cell lines from the HRI sgRNA#5 pool by single cell sorting on BD FACSJazz™. Cells were differentiated for 7 days for all data shown in this figure. In all panels error bars represent SEM; n=3 biological replicates. (**A**) Anti-HRI Western blot from lysates of two clonal HRI depleted cell lines and control cells. (**B**) HbF flow cytometry for HRI depleted clonal cell lines (gates were set on negative control as in Fig 2A). (**C**) RT-qPCR for globins for HRI depleted clonal cell lines, mean is shown ± standard error of the mean (SEM) from (n=3) biological replicates. (**D**) Primary transcripts of β-type globins. (**E**) mRNA levels of indicated genes.

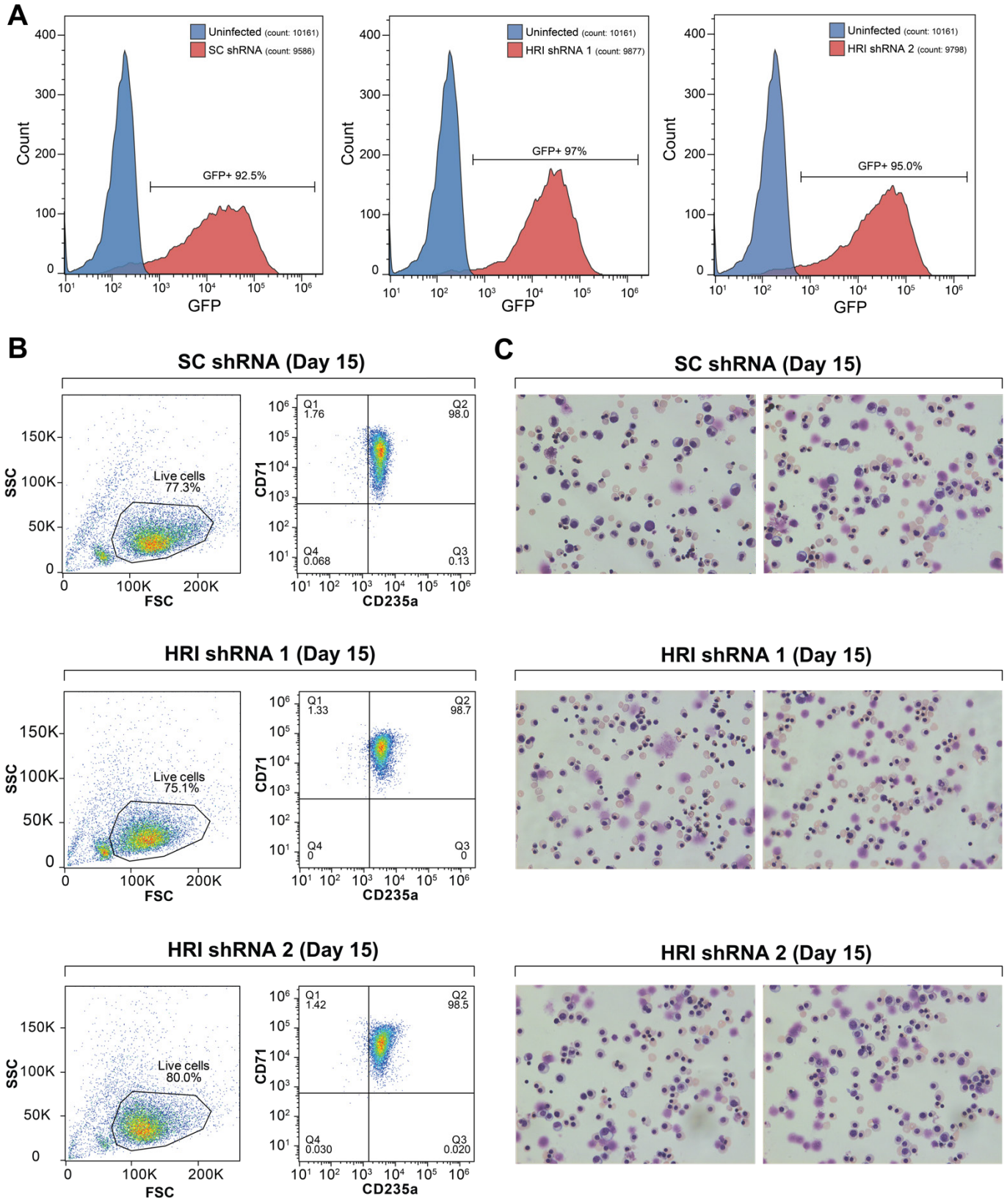

Fig. S11. Cell surface markers and cell morphology for HRI depleted CD34+ cells. (**A**) Representative transduction levels for shRNAs by GFP flow cytometry (Day 11). Uninfected were used as a gating control (blue) and compared to shRNA transduced populations (red). The uninfected control is the same for all panels shown. (**B**) Representative CD71/CD235a staining for SC shRNA and HRI shRNAs infected CD34+ cells at day 15 of culture. (**C**) Giemsa staining for SC shRNA control and HRI shRNAs infected CD34+ cells at day 15 of culture. 2 fields of view are shown for each sample.

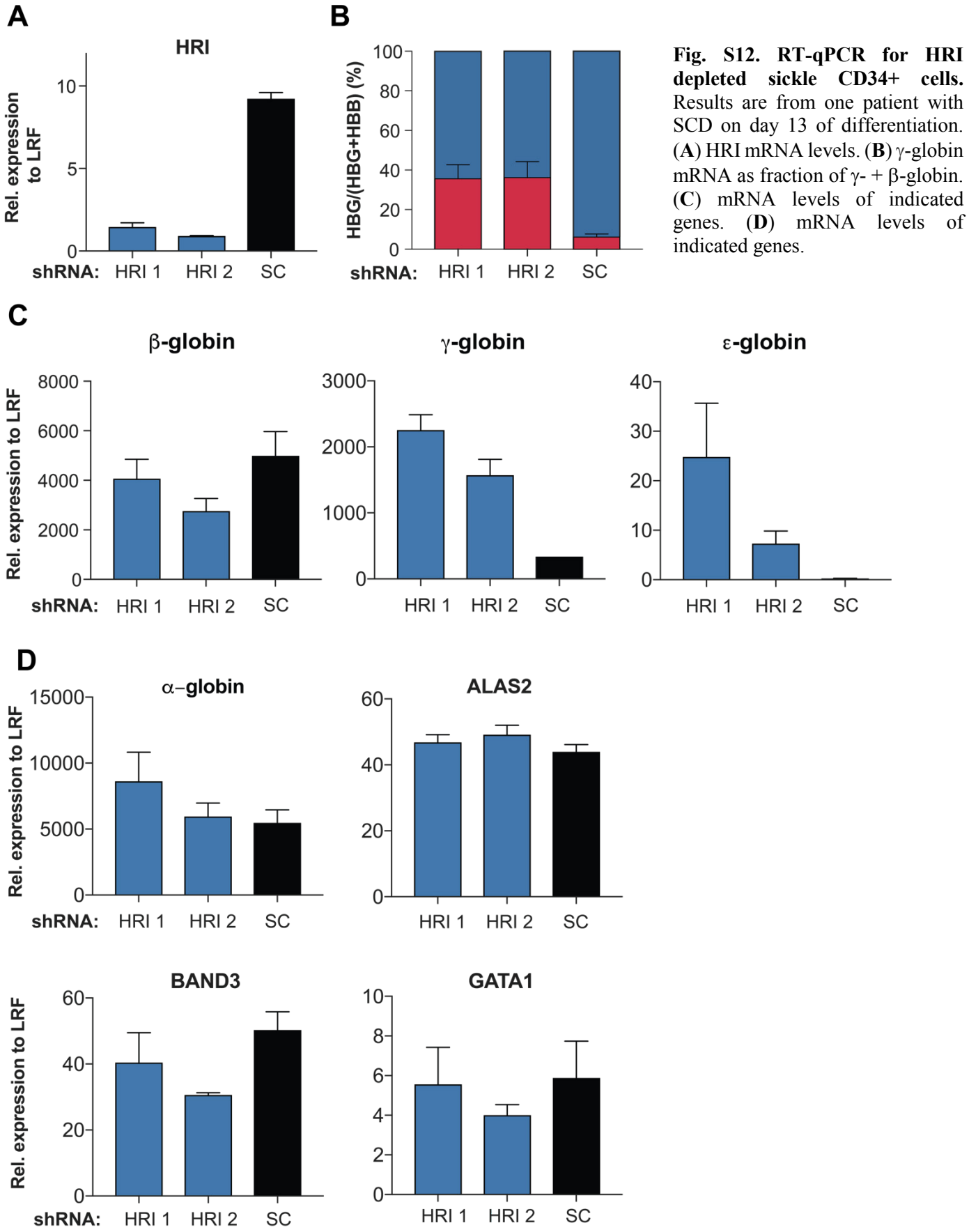

Fig. S12. RT-qPCR for HRI depleted sickle CD34+ cells. Results are from one patient with SCD on day 13 of differentiation. (**A**) HRI mRNA levels. (**B**) γ-globin mRNA as fraction of γ- + β-globin. (**C**) mRNA levels of indicated genes. (**D**) mRNA levels of indicated genes.

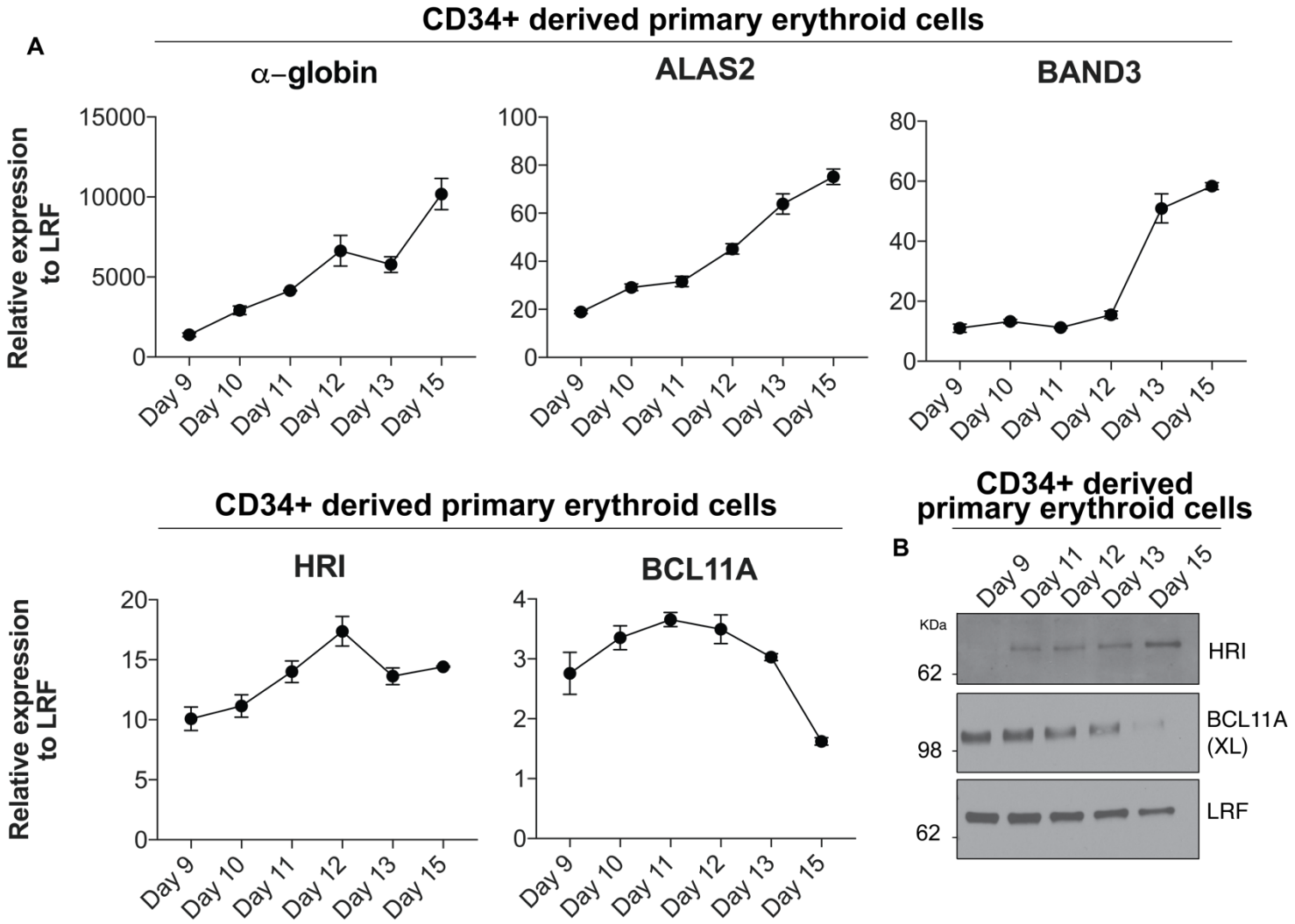

Fig. S13. HRI and BCL11A expression during erythroid maturation**.** (**A**) RT-qPCR for indicated primer sets for (n=2) technical replicates from one patient donor. Maturation markers α-globin, ALAS2 and BAND3 increase during erythroid maturation. HRI progressively increases during maturations. BCL11A increases early in maturation and then declines. (**B**) Western Blot for HRI, BCL11A and LRF during erythroid maturation. HRI increases in protein levels during maturation. BCL11A protein levels increase and then progressively decrease as shown previously (*29*). LRF remains relatively unchanged during maturation, as shown previously (*10*). These results suggest that BCL11A expression partly precedes HRI expression. The anti-correlated expression levels of HRI and BCL11A might appear in conflict with a requirement of HRI for BCL11A expression. However, please note that while HRI levels increase during erythroid maturation, its activity seems to decline as shown by western blots measuring eIF2α-P levels (Fig.2C), most likely due to the production of heme as a result of erythroid differentiation (*30*).

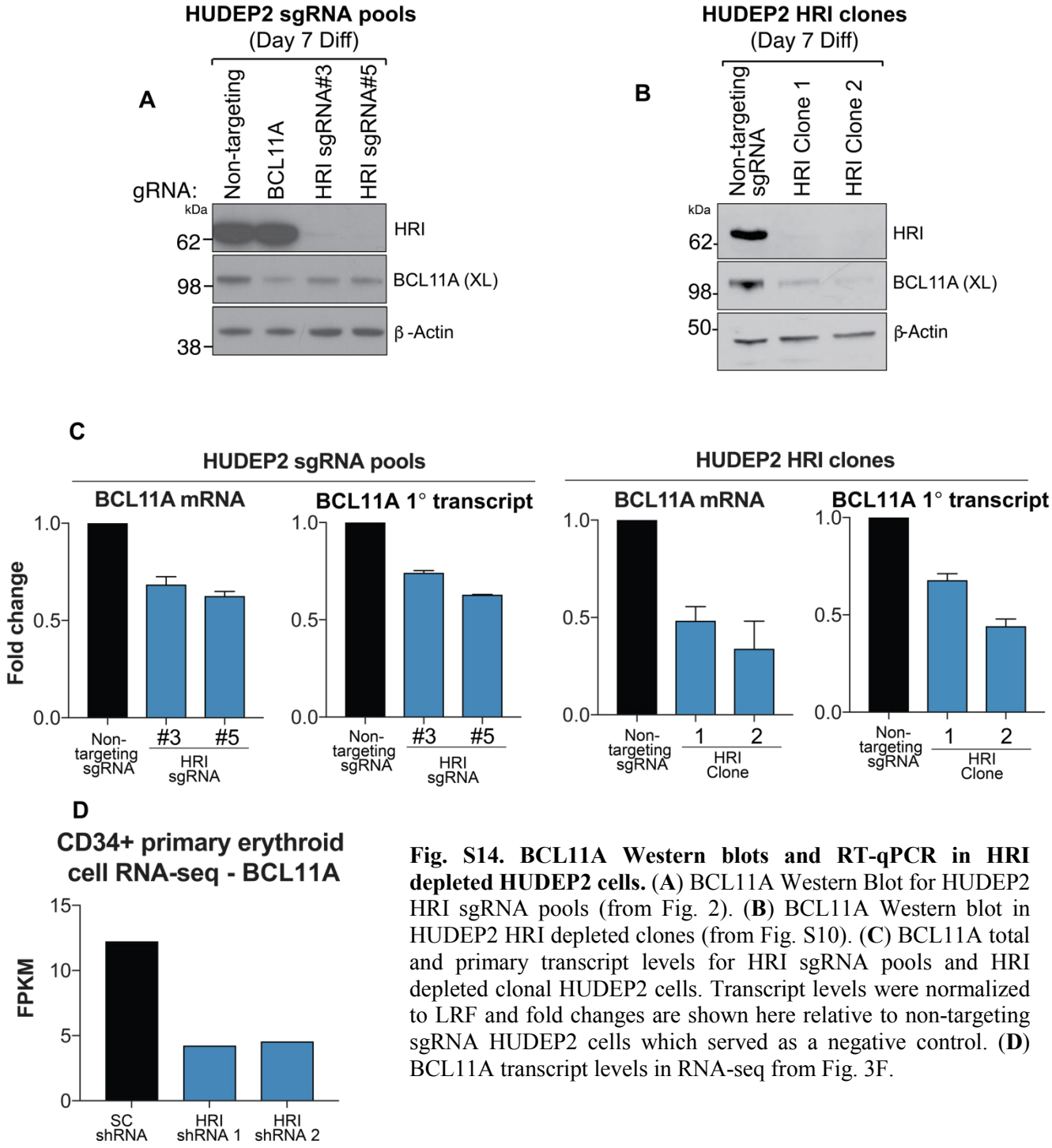

Fig. S14. BCL11A Western blots and RT-qPCR in HRI depleted HUDEP2 cells. (**A**) BCL11A Western Blot for HUDEP2 HRI sgRNA pools (from Fig. 2). (**B**) BCL11A Western blot in HUDEP2 HRI depleted clones (from Fig. S10). (**C**) BCL11A total and primary transcript levels for HRI sgRNA pools and HRI depleted clonal HUDEP2 cells. Transcript levels were normalized to LRF and fold changes are shown here relative to non-targeting sgRNA HUDEP2 cells which served as a negative control. (**D**) BCL11A transcript levels in RNA-seq from Fig. 3F.

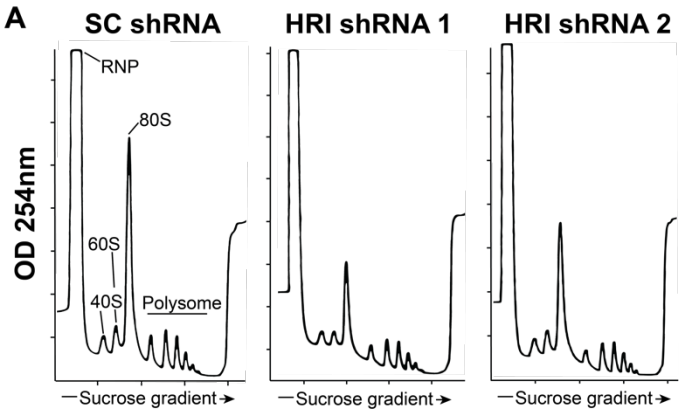

Fig. S15. Polysome profiling in primary erythroid cells. (**A**) Polysome tracings for shRNA transduced CD34+ erythroid cultures (Day 13). (**B**) Transcript abundances for each polysomal fraction normalized to spike-in control. (**C**) Transcript distribution across polysomal fractions. The proportion of transcripts for each fraction was determined by dividing the transcript abundance by the total amount of transcript across all the fractions (shown here as % of total). Polysome profiling was performed from cultures derived from (n=2) independent patient donors. Error bars are standard deviations for (n=2) technical replicates.

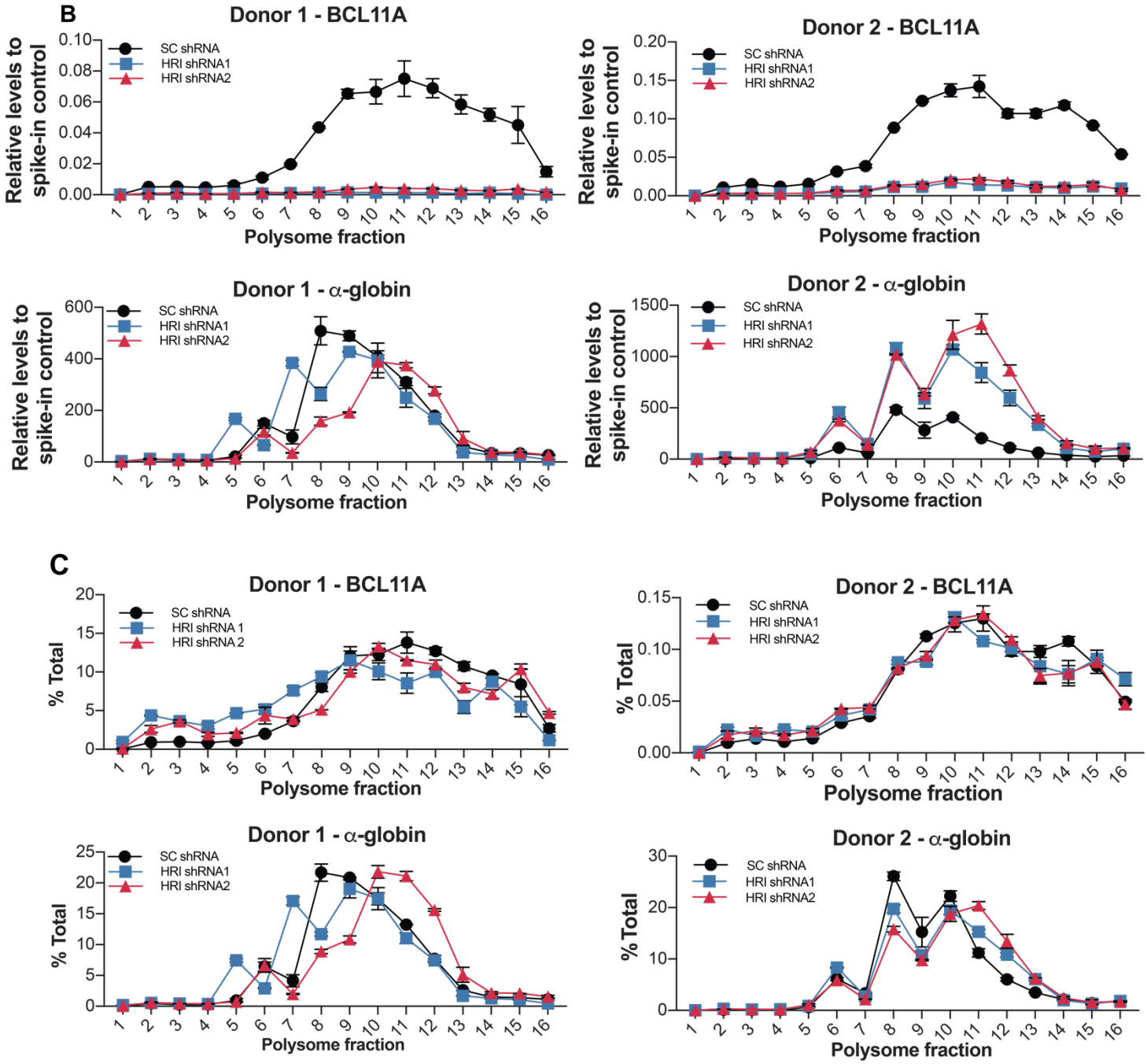

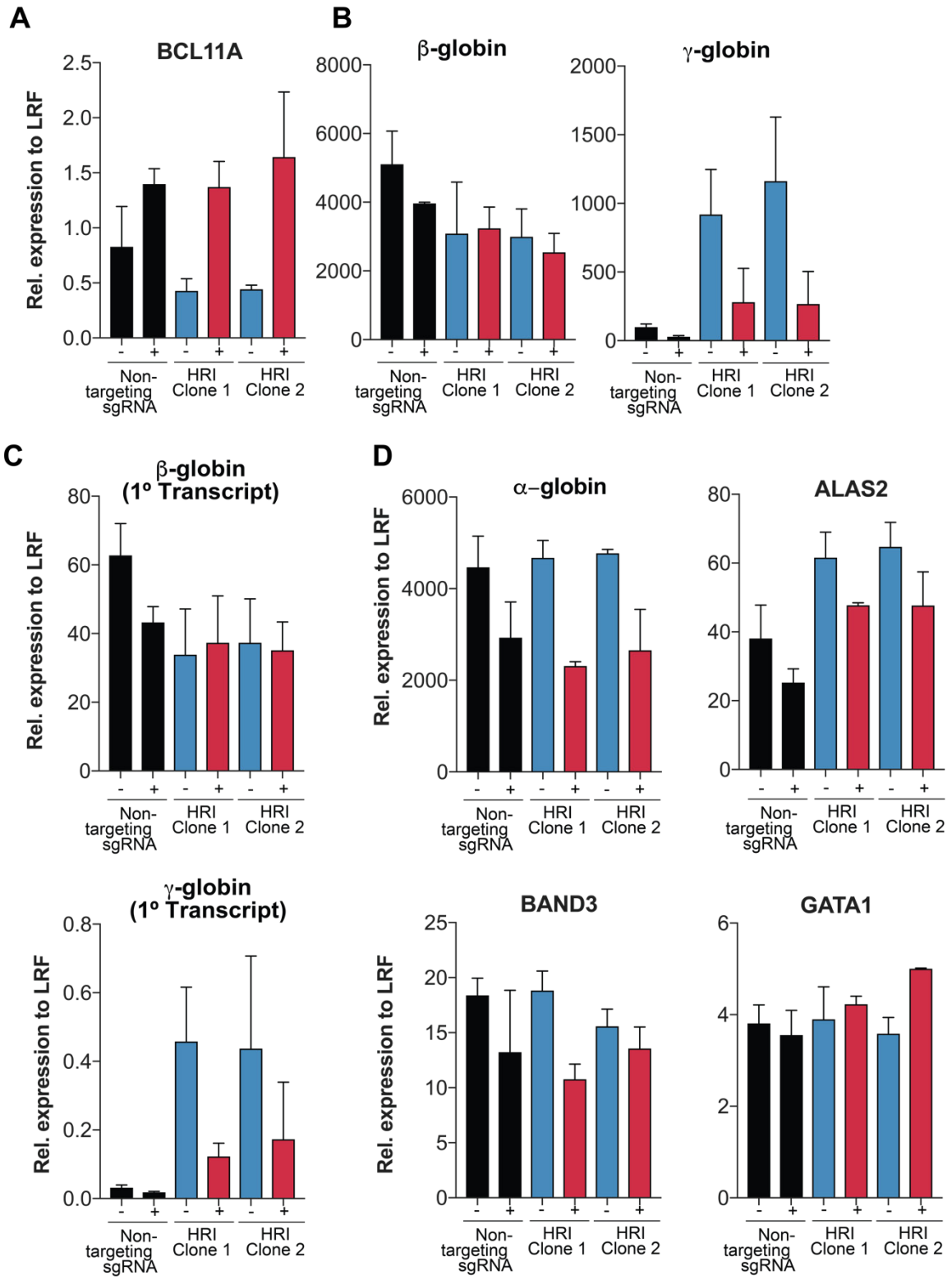

Fig. S16. Gene expression measurements in the BCL11A rescue experiments. Presence or absence of BCL11A cDNA is indicated by + or -, respectively. Cells were differentiated for 7 days for all data shown. Error bars: standard deviation from 2 biological replicates. (**A)** BCL11A transcript levels. While BCL11A transcripts were slightly higher in cells lines expressing exogenous BCL11A cDNA, they remained in a similar range to endogenous levels. (**B)** mRNA levels of indicated genes. BCL11A expression strongly reduced γ- and ε-globin transcript levels. (**C)** Primary-transcript levels of indicated genes. BCL11A expression strongly reduced γ-globin primary transcript levels. (**D)** Transcript levels for maturation markers. We note that expression BCL11A cDNA slightly reduced alpha-globin and BAND3 levels, but were not significantly different to levels from parental HUDEP2 cells.

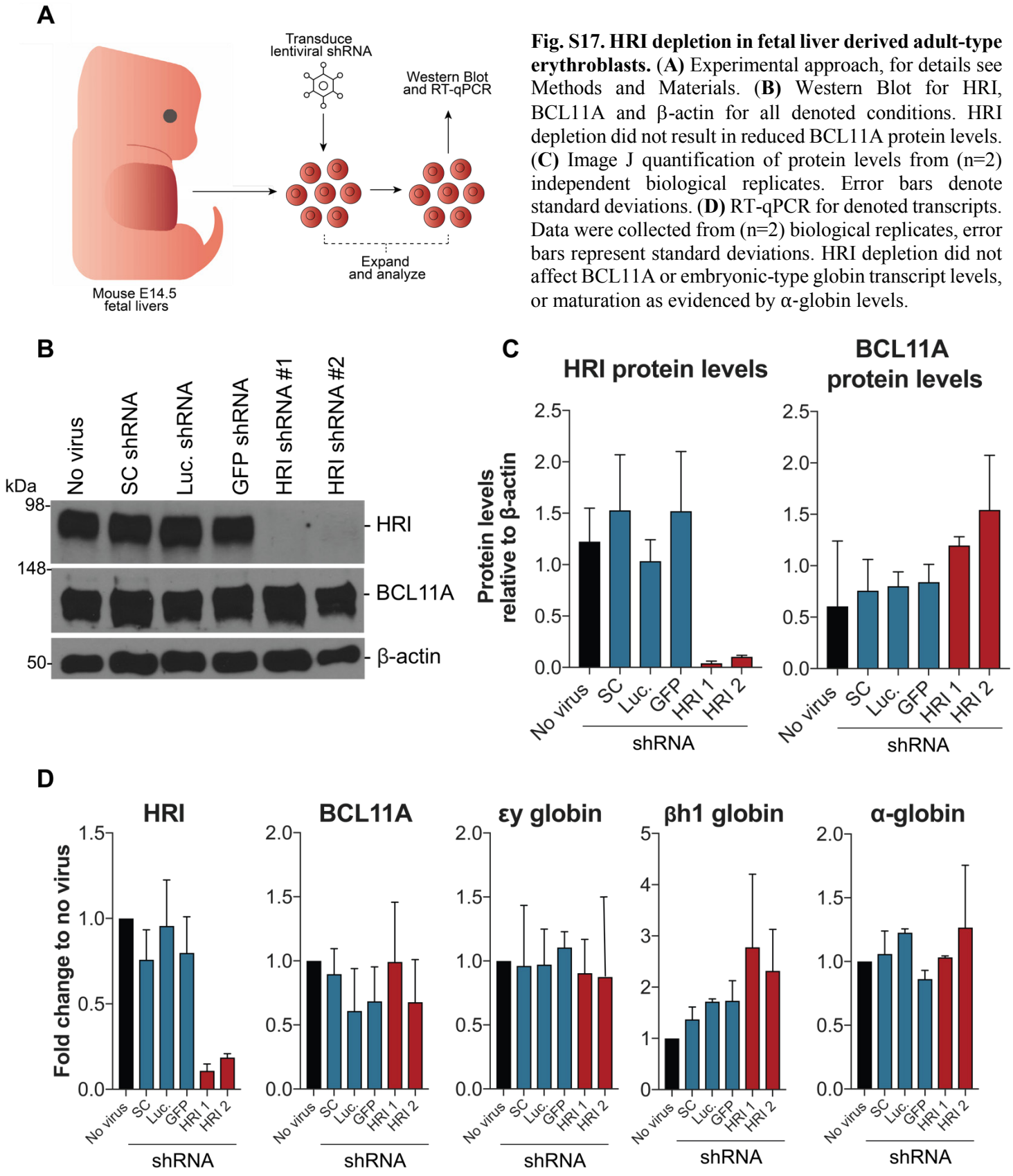

Fig. S17. HRI depletion in fetal liver derived adult-type erythroblasts. **(A)** Experimental approach, for details see Methods and Materials. **(B)** Western Blot for HRI, BCL11A and β-actin for all denoted conditions. HRI depletion did not result in reduced BCL11A protein levels. **(C)** Image J quantification of protein levels from (n=2) independent biological replicates. Error bars denote standard deviations. **(D)** RT-qPCR for denoted transcripts. Data were collected from (n=2) biological replicates, error bars represent standard deviations. HRI depletion did not affect BCL11A or embryonic-type globin transcript levels, or maturation as evidenced by α-globin levels.

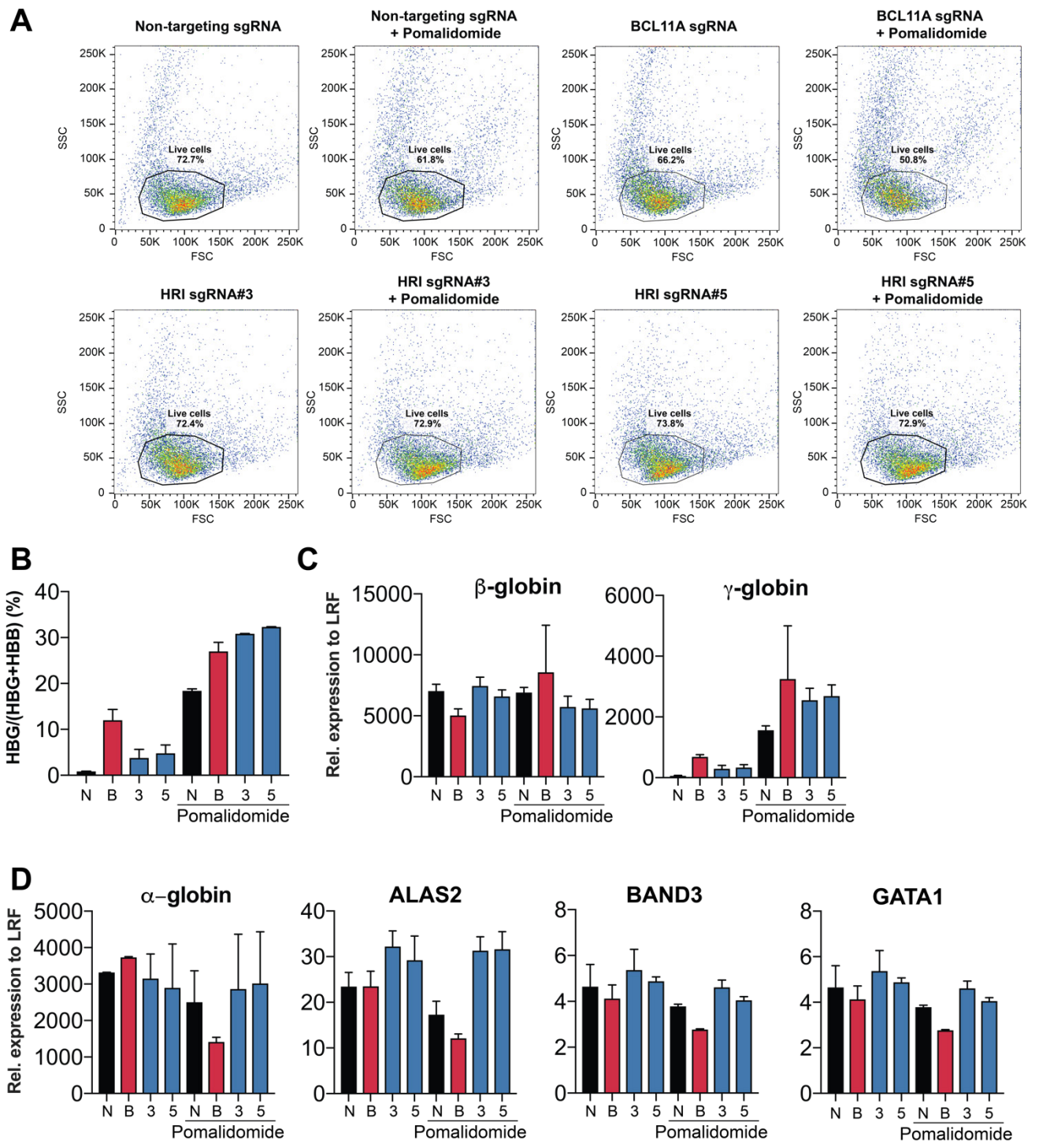

Fig. S18. Gene expression measurements in the pomalidomide combination experiments. Cells were differentiated for 7 days for all data shown with sgRNA HUDEP2-Cas9 pools. N denotes Non-targeting sgRNA, B denotes BCL11A sgRNA, 3 denotes HRI sgRNA #3, and 5 denotes HRI sgRNA#5. (**A**) Cell viability assessed by flow cytometry. (**B**) γ-globin mRNA as fraction of γ- + β-globin. (**C**) Globin profiles (mature transcripts) (**D**) mRNA levels of indicated genes. Error bars: standard deviation from 2 biological replicates. (**E**) Primary-transcript levels of indicated genes.

Protein Names	Gene Names	Protein abundance HRI sgRNA#5	Protein abundance non-targeting sgRNA	log2 (Fold Change)	p-value
Lariat debranching enzyme	DBR1	0.206	0.024	3.118	0.010
Hemoglobin subunit gamma-2	HBG2	100.998	12.559	3.008	0.003
Probable ATP-dependent RNA helicase YTHDC2	YTHDC2	0.077	0.014	2.493	0.010
Rab GTPase-activating protein 1-like, isoform 10	RABGAP1L	0.236	0.047	2.312	0.006
Alpha-hemoglobin-stabilizing protein	AHSP	646.580	174.552	1.889	0.004
Carbonic anhydrase 3	CA3	5.768	1.852	1.639	0.006
Angio-associated migratory cell protein	AAMP	1.361	0.452	1.591	0.006
Synaptosomal-associated protein 23	SNAP23	2.033	0.699	1.541	0.004
Heat shock 70 kDa protein 1B	HSPA1B	94.190	33.318	1.499	0.002
Selenium-binding protein 1	SELENBP1	17.385	7.014	1.310	0.003
Calcyclin-binding protein	CACYBP	20.810	9.323	1.158	0.008
Carbonic anhydrase 2	CA2	176.977	88.204	1.005	0.010

Table S1. Top differentially expressed proteins from HUDEP2 mass spectrometry.

Gene Name	Full Name	HRI sgRNA#5 mean count	Non-targeting sgRNA mean count	log2(Fold Change)	p-value (adjusted)
HBG2	hemoglobin subunit gamma 2	32957.50	4128.50	3.11	0
HBG1	hemoglobin subunit gamma 1	36346.00	4597.00	3.10	0
BGLT3	beta globin locus transcript 3 (non-protein coding)	285.00	14.50	2.69	6.16E-30
ESPN	espin	2434.00	589.50	2.11	1.43E-80
HBBP1	NA	2735.50	768.50	1.88	3.17E-50
FOSL2	FOS like 2, AP-1 transcription factor subunit	942.50	260.50	1.82	1.19E-31
IFIT1B	interferon induced protein with tetratricopeptide repeats 1B	1072.00	325.50	1.73	7.78E-32
RUNDC3A	RUN domain containing 3A	3079.50	1326.50	1.35	3.78E-40
KLHDC8B	kelch domain containing 8B	1549.50	667.00	1.30	2.98E-21
HIST2H2AA4	histone cluster 2 H2A family member a4	13544.50	6623.00	1.20	2.18E-65
MYL4	myosin light chain 4	2156.00	1166.50	1.03	8.04E-22
HIST1H2BB	histone cluster 1 H2B family member b	7694.00	4280.50	1.01	1.38E-42
HIST1H2BL	histone cluster 1 H2B family member l	6537.00	3626.00	1.01	1.72E-33
HIST1H2BG	histone cluster 1 H2B family member g	9231.00	5180.00	1.00	1.14E-38
REXO2	RNA exonuclease 2	4149.50	9857.50	-1.02	1.54E-30
ARG2	arginase 2	3213.00	8292.00	-1.13	9.90E-37
EIF2AK1	eukaryotic translation initiation factor 2 alpha kinase 1	17616.00	50037.00	-1.29	6.06E-121
TRIB3	tribbles pseudokinase 3	485.00	1824.50	-1.58	1.27E-32
SMN2	survival of motor neuron 2, centromeric	129.00	803.50	-1.95	1.28E-22
TNFRSF10B	TNF receptor superfamily member 10b	86.50	580.00	-2.01	2.82E-23

Table S2. Top differentially expressed transcripts from HUDEP2 RNA-seq.

Name	Sequence
BCL11A_Exon2_#1_F	CACCGTGAACCAGACCACGGCCCGT
BCL11A_Exon2_#1_R	AAACACGGGCCGTGGTCTGGTTCAC
BCL11A_Exon2_#2_F	CACCGCATCCAATCCCGTGGAGGT
BCL11A_Exon2_#2_R	AAACACCTCCACGGGATTGGATGC
BCL11A_+58_F	CACCGTTGCTTTTATCACAGGCTCC
BCL11A_+58_R	AAACGGAGCCTGTGATAAAAGCAAC
CHD4_Exon16_F	CACCGAACTCATTCTCTCGGATGA
CHD4_Exon16_R	AAACTCATCCGAGAGAATGAGTTC
CHD4_Exon17_F	CACCGCTGATTGTTCTTCAGCCGAT
CHD4_Exon17_R	AAACATCGGCTGAAGAACAATCAGC
CHD4_Exon22_F	CACCGAAATACGAACGCATCGATGG
CHD4_Exon22_R	AAACCCATCGATGCGTTCGTATTTC
EIF2AK1_sgRNA#1_F	CACCGTCTGGAAGTGCTCTCCGACC
EIF2AK1_sgRNA#1_R	AAACGGTCGGAGAGCACTTCCAGAC
EIF2AK1_sgRNA#2_F	CACCGTATCCACCTTTTCCTAAGA
EIF2AK1_sgRNA#2_R	AAACTCTTAGGAAAAGGTGGATAC
EIF2AK1_sgRNA#3_F	CACCGTTTTAGTTGCACCCTTAATC
EIF2AK1_sgRNA#3_R	AAACGATTAAGGGTGCAACTAAAAC
EIF2AK1_sgRNA#4_F	CACCGTTGTTGGCTATCACACCGCG
EIF2AK1_sgRNA#4_R	AAACCGCGGTGTGATAGCCAACAAC
EIF2AK1_sgRNA#5_F	CACCGATAGTCGAGAGAAACAAGCG
EIF2AK1_sgRNA#5_R	AAACCGCTTGTTTCTCTCGACTATC
EIF2AK1_sgRNA#6_F	CACCGTGGTGAACTTGAGTCGACCC
EIF2AK1_sgRNA#6_R	AAACGGGTCGACTCAAGTTCACCAC
Non_targeting_sgRNA_F	CACCGACCGGAACGATCTCGCGTA
Non_targeting_sgRNA_R	AAACTACGCGAGATCGTTCCGGTC

Table S3. Oligos for sgRNAs.

Name	Sequence
BCL11A_Exon2_#1_TIDE_F	ATGCAAACAGCTTTTCTCCTTGC
BCL11A_Exon2_#1_TIDE_R	CACATTTGTTGCTGTGGGTGTG
BCL11A_Exon2_#2_TIDE_F	CCAGAGAGAAGGTGTCTGATGTGT
BCL11A_Exon2_#2_TIDE_R	AGATGTGCTTCTCCCCTTTCTGTC
BCL11A_+58_TIDE_F	GTAGCTGGTACCTGATAGGTGCC
BCL11A_+58_TIDE_R	GGAAAACAGCCTGACTGTGCC
CHD4_Exon16_TIDE_F	GAGCCCAAAATAGCCATGTCAATG
CHD4_Exon16_TIDE_R	TGTAGTTATGGTGGGACCTTGGG
CHD4_Exon17_TIDE_F	GTGCTGGAGTGAGTAACCATTCAAT
CHD4_Exon17_TIDE_R	CGCATGAAGGTATCTCAGGGGA
CHD4_Exon22_TIDE_F	GCTATTTGAGCTTGAACAAGTCCTGAC
CHD4_Exon22_TIDE_R	TGTTCTCAGGAAGCTCCTAAGATGC

Table S4. Primers used for TIDE assays shown in Fig. S2.

Name	Sequence
HRI_shRNA1_F	CACCGGCAGAGAGCAATGTGGTGTTAACTCGAGTTAACACCACATTGCTCTCTGTTTTTG
HRI_shRNA1_R	AATTCAAAAACAGAGAGCAATGTGGTGTTAACTCGAGTTAACACCACATTGCTCTCTGCC
HRI_shRNA4_F	CACCGGGCAGAAGTTCTAACAGGTTTACTCGAGTAAACCTGTTAGAACTTCTGCTTTTTG
HRI_shRNA4_R	AATTCAAAAAGCAGAAGTTCTAACAGGTTTACTCGAGTAAACCTGTTAGAACTTCTGCCC
LRF_shRNA_F	CACCGGCCACTGAGACACAAACCTATTCTCGAGAATAGGTTTGTGTCTCAGTGGTTTTTG
LRF_shRNA_R	AATTCAAAAACCACTGAGACACAAACCTATTCTCGAGAATAGGTTTGTGTCTCAGTGGCC
SC_shRNA_F	CACCGGCAACAAGATGAAGAGCACCAACTCGAGTTGGTGCTCTTCATCTTGTTGTTTTTG
SC_shRNA_R	AATTCAAAAACAACAAGATGAAGAGCACCAACTCGAGTTGGTGCTCTTCATCTTGTTGCC
Luciferase_shRNA_F	CACCGGCGCTGAGTACTTCGAAATGTCCTCGAGGACATTTCGAAGTACTCAGCGTTTTTG
Luciferase_shRNA_R	AATTCAAAAACGCTGAGTACTTCGAAATGTCCTCGAGGACATTTCGAAGTACTCAGCGCC
TurboGFP_shRNA_F	CACCGGCGTGATCTTCACCGACAAGATCTCGAGATCTTGTCGGTGAAGATCACGTTTTTG
TurboGFP_shRNA_R	AATTCAAAAACGTGATCTTCACCGACAAGATCTCGAGATCTTGTCGGTGAAGATCACGCC
mHRI_shRNA_1_F	CACCGGTGGTGTTAAAGATAATGAAAGCTCGAGCTTTCATTATCTTTAACACCATTTTTG
mHRI_shRNA_1_R	AATTCAAAAATGGTGTTAAAGATAATGAAAGCTCGAGCTTTCATTATCTTTAACACCACC
mHRI_shRNA_2_F	CACCGGCAGCCATTCGGGACAGAAATGCTCGAGCATTTCTGTCCCGAATGGCTGTTTTTG
mHRI_shRNA_2_R	AATTCAAAAACAGCCATTCGGGACAGAAATGCTCGAGCATTTCTGTCCCGAATGGCTGCC

Table S5. shRNA oligos.

Name	Sequence
LRG_F2	TCTTGTGGAAAGGACGAAACACCG
LRG_R2	TCTACTATTCTTTCCCCTGCACTGT
PE-5	AATGATACGGCGACCACCGAGATCTACACTCTTTCCCTACACGACGCTCTTCCGATCT
PE-7	CAAGCAGAAGACGGCATACGAGATCGGTCTCGGCATTCCTGCTGAACCGCTCTTCCGATCT

Table S6. sgRNA sequencing library primers.

Name	Sequence
Gamma_globin_F	TGGCAAGAAGGTGCTGACTTC
Gamma_globin_R	GCAAAGGTGCCCTTGAGATC
Beta_globin_F	TGGGCAACCCTAAGGTGAAG
Beta_globin_R	GTGAGCCAGGCCATCACTAAA
Alpha_globin_F	AAGACCTACTTCCCGCACTTC
Alpha_globin_R	GTTGGGCATGTCGTCCAC
Gamma_globin_PT_F	TTTGTGGCACCTTCTGACTG
Gamma_globin_PT_R	GCCAAAGCTGTCAAAGAA
Beta_globin_PT_F	GCTAGGCCCTTTTGCTAATC
Beta_globin_PT_R	CTGGTGGGGTGAATTCTT
ALAS2_F	CAGCGCAATGTCAAGCAC
ALAS2_R	TAGATGCCATGCTTGGAGAG
BAND3_F	ACCTCTCTCACCTCACCTTCTG
BAND3_R	AACCTGTCTAGCAGTTGGTTGG
GATA1_F	CTGTCCCCAATAGTGCTTATGG
GATA1_R	GAATAGGCTGCTGAATTGAGGG
HRI_F	CACCCGAACAGTTGGAAGGA
HRI_R	AGAGCTCTAGCAGGACCACA
BCL11A_F	ACAAACGGAAACAATGCAATGG
BCL11A_R	TTTCATCTCGATTGGTGAAGGG
ZBTB7A_F	GCTTGGGCCGGTTGAATGTA
ZBTB7A_R	GGCTGTGAAGTTACCGTCGG
Mouse_HRI_F	CTGCTGCAGAGTGAGCTTTTTC
Mouse_HRI_R	CTGAGAAAGGAGGCTTAGTTGC
Mouse_Bcl11a_F	GCCCCAAACAGGAACACATA
Mouse_Bcl11a_R	GGGGCATATTCTGCACTCAT
Mouse_ey-globin_F	ACAGCTTTGGGAACTTGTCCTC
Mouse_ey-globin_R	TCTCCAAAAGCAGTCAGCACC
Mouse_bh1-globin_F	AGGCAGCTATCACAAGCATCTG
Mouse_bh1-globin_R	AACTTGTCAAAGAATCTCTGAGTCCA
Bactin_F	ACACCCGCCACCAGTTC
Bactin_R	TACAGCCCGGGGAGCAT

Table S7. RT-qPCR primers.

References and Notes

1. V. G. Sankaran, S. H. Orkin, The switch from fetal to adult hemoglobin. *Cold Spring Harb. Perspect. Med.* **3**, a011643 (2013). doi:10.1101/cshperspect.a011643 Medline

2. O. S. Platt, D. J. Brambilla, W. F. Rosse, P. F. Milner, O. Castro, M. H. Steinberg, P. P. Klug, Mortality in sickle cell disease. Life expectancy and risk factors for early death. *N. Engl. J. Med.* **330**, 1639–1644 (1994). doi:10.1056/NEJM199406093302303 Medline

3. A. Basak, M. Hancarova, J. C. Ulirsch, T. B. Balci, M. Trkova, M. Pelisek, M. Vlckova, K. Muzikova, J. Cermak, J. Trka, D. A. Dyment, S. H. Orkin, M. J. Daly, Z. Sedlacek, V. G. Sankaran, BCL11A deletions result in fetal hemoglobin persistence and neurodevelopmental alterations. *J. Clin. Invest.* **125**, 2363–2368 (2015). doi:10.1172/JCI81163 Medline

4. V. G. Sankaran, T. F. Menne, J. Xu, T. E. Akie, G. Lettre, B. Van Handel, H. K. A. Mikkola, J. N. Hirschhorn, A. B. Cantor, S. H. Orkin, Human fetal hemoglobin expression is regulated by the developmental stage-specific repressor BCL11A. *Science* **322**, 1839–1842 (2008). doi:10.1126/science.1165409 Medline

5. V. G. Sankaran, J. Xu, T. Ragoczy, G. C. Ippolito, C. R. Walkley, S. D. Maika, Y. Fujiwara, M. Ito, M. Groudine, M. A. Bender, P. W. Tucker, S. H. Orkin, Developmental and species-divergent globin switching are driven by BCL11A. *Nature* **460**, 1093–1097 (2009). doi:10.1038/nature08243 Medline

6. J. Xu, C. Peng, V. G. Sankaran, Z. Shao, E. B. Esrick, B. G. Chong, G. C. Ippolito, Y. Fujiwara, B. L. Ebert, P. W. Tucker, S. H. Orkin, Correction of sickle cell disease in adult mice by interference with fetal hemoglobin silencing. *Science* **334**, 993–996 (2011). doi:10.1126/science.1211053 Medline

7. A. Perumbeti, T. Higashimoto, F. Urbinati, R. Franco, H. J. Meiselman, D. Witte, P. Malik, A novel human gamma-globin gene vector for genetic correction of sickle cell anemia in a humanized sickle mouse model: Critical determinants for successful correction. *Blood* **114**, 1174–1185 (2009). doi:10.1182/blood-2009-01-201863 Medline

8. D. E. Bauer, S. C. Kamran, S. Lessard, J. Xu, Y. Fujiwara, C. Lin, Z. Shao, M. C. Canver, E. C. Smith, L. Pinello, P. J. Sabo, J. Vierstra, R. A. Voit, G.-C. Yuan, M. H. Porteus, J. A. Stamatoyannopoulos, G. Lettre, S. H. Orkin, An erythroid enhancer of BCL11A subject to genetic variation determines fetal hemoglobin level. *Science* **342**, 253–257 (2013). doi:10.1126/science.1242088 Medline

9. S. M. Bakanay, E. Dainer, B. Clair, A. Adekile, L. Daitch, L. Wells, L. Holley, D. Smith, A. Kutlar, Mortality in sickle cell patients on hydroxyurea therapy. *Blood* **105**, 545–547 (2005). doi:10.1182/blood-2004-01-0322 Medline

10. T. Masuda, X. Wang, M. Maeda, M. C. Canver, F. Sher, A. P. W. Funnell, C. Fisher, M. Suciu, G. E. Martyn, L. J. Norton, C. Zhu, R. Kurita, Y. Nakamura, J. Xu, D. R. Higgs, M. Crossley, D. E. Bauer, S. H. Orkin, P. V. Kharchenko, T. Maeda, Transcription factors LRF and BCL11A independently repress expression of fetal hemoglobin. *Science* **351**, 285–289 (2016). doi:10.1126/science.aad3312 Medline

11. G. Manning, D. B. Whyte, R. Martinez, T. Hunter, S. Sudarsanam, The protein kinase complement of the human genome. *Science* **298**, 1912–1934 (2002). doi:10.1126/science.1075762 Medline

12. J. Shi, E. Wang, J. P. Milazzo, Z. Wang, J. B. Kinney, C. R. Vakoc, Discovery of cancer drug targets by CRISPR-Cas9 screening of protein domains. *Nat. Biotechnol.* **33**, 661–667 (2015). doi:10.1038/nbt.3235 Medline

13. R. Kurita, N. Suda, K. Sudo, K. Miharada, T. Hiroyama, H. Miyoshi, K. Tani, Y. Nakamura, Establishment of immortalized human erythroid progenitor cell lines able to produce enucleated red blood cells. *PLOS ONE* **8**, e59890–e15 (2013). doi:10.1371/journal.pone.0059890 Medline

14. M. C. Canver, E. C. Smith, F. Sher, L. Pinello, N. E. Sanjana, O. Shalem, D. D. Chen, P. G. Schupp, D. S. Vinjamur, S. P. Garcia, S. Luc, R. Kurita, Y. Nakamura, Y. Fujiwara, T. Maeda, G.-C. Yuan, F. Zhang, S. H. Orkin, D. E. Bauer, BCL11A enhancer dissection by Cas9-mediated in situ saturating mutagenesis. *Nature* **527**, 192–197 (2015). doi:10.1038/nature15521 Medline

15. J.-J. Chen, Translational control by heme-regulated eIF2α kinase during erythropoiesis. *Curr. Opin. Hematol.* **21**, 172–178 (2014). doi:10.1097/MOH.0000000000000030 Medline

16. B. M. Dulmovits, A. O. Appiah-Kubi, J. Papoin, J. Hale, M. He, Y. Al-Abed, S. Didier, M. Gould, S. Husain-Krautter, S. A. Singh, K. W. H. Chan, A. Vlachos, S. L. Allen, N. Taylor, P. Marambaud, X. An, P. G. Gallagher, N. Mohandas, J. M. Lipton, J. M. Liu, L. Blanc, Pomalidomide reverses γ-globin silencing through the transcriptional reprogramming of adult hematopoietic progenitors. *Blood* **127**, 1481–1492 (2016). doi:10.1182/blood-2015-09-667923 Medline

17. C. K. Hahn, C. H. Lowrey, Eukaryotic initiation factor 2α phosphorylation mediates fetal hemoglobin induction through a post-transcriptional mechanism. *Blood* **122**, 477–485 (2013). doi:10.1182/blood-2013-03-491043 Medline

18. C. K. Hahn, C. H. Lowrey, Induction of fetal hemoglobin through enhanced translation efficiency of γ-globin mRNA. *Blood* **124**, 2730–2734 (2014). doi:10.1182/blood-2014-03-564302 Medline

19. A. P. Han, C. Yu, L. Lu, Y. Fujiwara, C. Browne, G. Chin, M. Fleming, P. Leboulch, S. H. Orkin, J. J. Chen, Heme-regulated eIF2α kinase (HRI) is required for translational regulation and survival of erythroid precursors in iron deficiency. *EMBO J.* **20**, 6909–6918 (2001). doi:10.1093/emboj/20.23.6909 Medline

20. S. Liu, S. Bhattacharya, A. Han, R. N. V. S. Suragani, W. Zhao, R. C. Fry, J.-J. Chen, Haem-regulated eIF2α kinase is necessary for adaptive gene expression in erythroid precursors under the stress of iron deficiency. *Br. J. Haematol.* **143**, 129–137 (2008). doi:10.1111/j.1365-2141.2008.07293.x Medline

21. S. Liu, R. N. V. S. Suragani, A. Han, W. Zhao, N. C. Andrews, J.-J. Chen, Deficiency of heme-regulated eIF2α kinase decreases hepcidin expression and splenic iron in *HFE*$^{-/-}$ mice. *Haematologica* **93**, 753–756 (2008). doi:10.3324/haematol.12175 Medline

22. E. K. Brinkman, T. Chen, M. Amendola, B. van Steensel, Easy quantitative assessment of genome editing by sequence trace decomposition. *Nucleic Acids Res.* **42**, e168–e168 (2014). doi:10.1093/nar/gku936 Medline

23. P. D. Hsu, D. A. Scott, J. A. Weinstein, F. A. Ran, S. Konermann, V. Agarwala, Y. Li, E. J. Fine, X. Wu, O. Shalem, T. J. Cradick, L. A. Marraffini, G. Bao, F. Zhang, DNA targeting specificity of RNA-guided Cas9 nucleases. *Nat. Biotechnol.* **31**, 827–832 (2013). doi:10.1038/nbt.2647 Medline

24. J. Cox, M. Mann, MaxQuant enables high peptide identification rates, individualized p.p.b.-range mass accuracies and proteome-wide protein quantification. *Nat. Biotechnol.* **26**, 1367–1372 (2008). doi:10.1038/nbt.1511 Medline

25. H. Nishimasu, F. A. Ran, P. D. Hsu, S. Konermann, S. I. Shehata, N. Dohmae, R. Ishitani, F. Zhang, O. Nureki, Crystal structure of Cas9 in complex with guide RNA and target DNA. *Cell* **156**, 935–949 (2014). doi:10.1016/j.cell.2014.02.001 Medline

26. B. Chen, L. A. Gilbert, B. A. Cimini, J. Schnitzbauer, W. Zhang, G.-W. Li, J. Park, E. H. Blackburn, J. S. Weissman, L. S. Qi, B. Huang, Dynamic imaging of genomic loci in living human cells by an optimized CRISPR/Cas system. *Cell* **155**, 1479–1491 (2013). doi:10.1016/j.cell.2013.12.001 Medline

27. J. Xu, D. E. Bauer, M. A. Kerenyi, T. D. Vo, S. Hou, Y.-J. Hsu, H. Yao, J. J. Trowbridge, G. Mandel, S. H. Orkin, Corepressor-dependent silencing of fetal hemoglobin expression by BCL11A. *Proc. Natl. Acad. Sci. U.S.A.* **110**, 6518–6523 (2013). doi:10.1073/pnas.1303976110 Medline

28. N. Novershtern, A. Subramanian, L. N. Lawton, R. H. Mak, W. N. Haining, M. E. McConkey, N. Habib, N. Yosef, C. Y. Chang, T. Shay, G. M. Frampton, A. C. B. Drake, I. Leskov, B. Nilsson, F. Preffer, D. Dombkowski, J. W. Evans, T. Liefeld, J. S. Smutko, J. Chen, N. Friedman, R. A. Young, T. R. Golub, A. Regev, B. L. Ebert, Densely interconnected transcriptional circuits control cell states in human hematopoiesis. *Cell* **144**, 296–309 (2011). doi:10.1016/j.cell.2011.01.004 Medline

29. J. Xu, V. G. Sankaran, M. Ni, T. F. Menne, R. V. Puram, W. Kim, S. H. Orkin, Transcriptional silencing of γ-globin by BCL11A involves long-range interactions and cooperation with SOX6. *Genes Dev.* **24**, 783–798 (2010). doi:10.1101/gad.1897310 Medline

30. Z. Yang, S. B. Keel, A. Shimamura, L. Liu, A. T. Gerds, H. Y. Li, B. L. Wood, B. L. Scott, J. L. Abkowitz, Delayed globin synthesis leads to excess heme and the macrocytic anemia of Diamond Blackfan anemia and del(5q) myelodysplastic syndrome. *Sci. Transl. Med.* **8**, 338ra67 (2016). doi:10.1126/scitranslmed.aaf3006 Medline